Abstract Extraordinary optical transmission through an array of holes in a metal film was reported by Ebbesen and coworkers in 1998. Since that work there has been abundant research activity aimed at understanding the physics and at the development of the many applications associated with this phenomenon, hence the topic of this review. The study of hole-arrays in a metal is not new – theoretical contributions on a small-hole array date back to Lord Rayleigh's description of Wood's anomaly in 1907 and there has been considerable research on metal meshes and hole-arrays since 1962. Bethe's theory, adapted to treat hole-arrays, is the simplest theoretical description of the transmission resonance. Following a description of this basic theory, we present the research on the additional effects from variations in real metal properties at different wavelengths, film thickness, hole-shape and lattice configuration. The many promising applications being developed using hole-arrays are examined, including polarization control, filtering, switching, nonlinear optics, surface plasmon resonance sensing, surface-enhanced fluorescence, surface-enhanced Raman scattering, absorption spectroscopy, and quantum interactions. Finally, the various approaches, developments in hole-array fabrication, and integration of hole-arrays into devices are described.

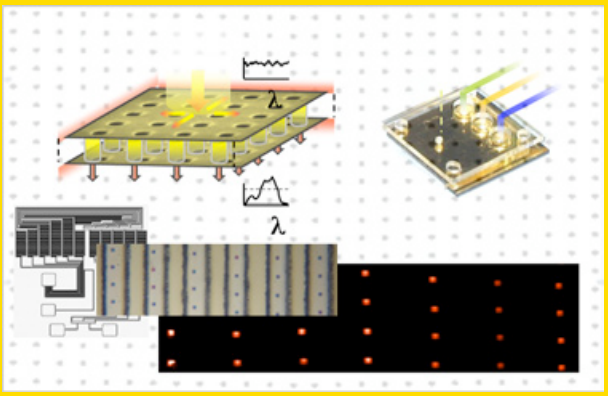

(top left) Schematic of resonant transmission through nanohole array using scanning electron microscope image of as-fabricated sample. (top right) Microfluidic chip incorporating nanohole arrays. (bottom) Composite image of array of nanohole arrays used as sensors in a immunoassay-like microfluidic device, showing (left to right) schematic of microfluidic layout, microscope image of arrays in microfluidic channels, and laser transmission modified by adsorbed molecules.

Resonant optical transmission through hole-arrays in metal films: physics and applications

Reuven Gordon[1,*], *Alexandre G. Brolo*[2], *David Sinton*[3], *and Karen L. Kavanagh*[4]

[1] Department of Electrical and Computer Engineering, University of Victoria, P. O. Box 3055, Victoria, B. C. V8W 3P6, Canada
[2] Department of Chemistry, University of Victoria, P. O. Box 3065, Victoria, B. C. V8W 3V6, Canada
[3] Department of Mechanical Engineering, University of Victoria, P. O. Box 3055, Victoria, B. C. V8W 3P6, Canada
[4] Department of Physics, Simon Fraser University, 8888 University Drive, Burnaby, B. C. V5A 1S6, Canada

Received: 19 December 2008, Revised: 9 March 2009, Accepted: 27 March 2009
Published online: 11 May 2009

Key words: Surface plasmons, nanophotonics, gratings, surface waves, apertures, diffraction, optics of metals.

PACS: 78.66.Bz, 78.67.-n, 78.68.+m, 42.79.-e, 42.79.Ag, 42.79.Dj

1. Introduction

In 1907, Lord Rayleigh explained the anomalous absorption of gratings that had been observed by Prof. Wood, and that are commonly referred to as Wood's Anomaly [1]. In doing so, he considered the transmission of light through a linear array of small holes in a thin metal sheet, and his finding was that when the hole-spacing approached the wavelength, there could be no transmission. He did not consider the unusual resonance in transmission that results for wavelengths just longer than the array-period, which will be the primary focus of this work.

The theory of transmission through a single hole in a metal was given by Bethe in 1944 [2], and later extended by Bouwkamp [3]. In Bethe's theory, the transmission through

* Corresponding author: e-mail: rgordon@uvic.ca

a hole dropped as the fourth power of the hole-diameter for small holes. Therefore, many expected that almost no light would emerge from an array of small holes.

There were a number of works investigating larger holes in metal meshes, starting in 1962 [4]. In those works, typically in the infrared, a strong transmission resonance was observed for wavelengths just longer than the array periodicity. Several theoretical works described the origin of this phenomenon; however, there was no clear description of how the transmission would behave for smaller holes. At that time, many applications of the metal meshes were already recognized.

With the advent of nanotechnology, it has become possible to make holes smaller than the wavelength of visible light. Early works produced arrays of holes by electron-beam lithography, and although they noted considerable transmission, no resonant effects were found with hole-periodicity [5,6]. In 1998, Ebbesen and co-workers reported on the extraordinary optical transmission (EOT) through arrays of holes made by focused-ion beam milling through various metals, even when the holes were much smaller than the optical wavelength [7]. Their work led to an explosion of activity in the optical properties of nanostructured metals and a resurgence of research in the transmission properties of hole-arrays throughout the electromagnetic spectrum.

A decade having past, with nearly 2000 indexed citations to Ebbesen's original paper, the activity has not diminished. The theoretical understanding of EOT has advanced considerably, including studies on the role of material response at different wavelengths, and geometric properties, such as film-thickness, hole-shape and lattice arrangement. Furthermore, a great number of applications have emerged for hole-arrays due to their resonant subwavelength light confinement and transmission. These applications include optical filters, polarizers, nonlinear optics, sensing and spectroscopy. There is great potential for additional growth in each of these areas, as well as expansion into the fields of quantum optics and subwavelength imaging. The ability to fabricate subwavelength hole-arrays has also advanced, and it is now possible to create nanoscale holes over large substrates with high-throughput and inexpensive techniques, such as imprint lithography and interference lithography. With these advances, many groups are integrating hole-arrays into devices; for example, including microfluidics, light sources and detectors.

The purpose of this review is to present a succinct yet broad coverage of the work concerning hole-arrays in metal films. Several excellent reviews have been presented that cover parts of this topic already, ranging from in-depth coverage of the physics for experts [8] to popular reviews aimed at a general science audience [9]. There have been many reviews focused on specific applications, such as sensing and spectroscopy [10–12] and still more on fabrication technologies. In the context of all of these excellent works, our goal is to focus particularly on hole-arrays, yet provide an in-depth review of the associated physics, applications, fabrication and device integration.

2. Physics of hole-arrays in a metal thin film

2.1. Transmission through a small hole

In 1944, Bethe considered the electromagnetic transmission through an aperture in a perfectly conducting infinitely thin screen [2]. The aperture was much smaller than the wavelength, so that the phase-shift associated with wave propagation was ignored. For this subwavelength limit, the problem is reduced to one of electrostatics. In this regime, Bethe showed that the aperture could be treated as a magnetic dipole. It has the same magnetic polarizability as a capacitor plate with a hole in it for a constant applied field [13]. From Bethe's calculations, the transmission (normalized to hole-area) through the hole diminishes rapidly as the fourth power of the ratio between the aperture size and the wavelength; small holes transmit almost no light. A more detailed consideration of the field distribution in the near-field of the aperture was presented by Bouwkamp [3]; hence the common reference to Bethe-Bouwkamp's aperture theory.

It should be emphasized that Bethe's original theory was for a single small hole in an infinitely thin metal treated as a perfect electric conductor. It was not for an array of holes, or for holes comparable to the wavelength in size. For real metals of finite thickness, we must also consider the propagation or decay of the waveguide modes inside the aperture leading to resonances, as will be described in Sect. 2.5. It is also found within the effective index approximation [14] that the cutoff wavelength is larger for smaller holes due to interaction with the plasmons in the metal. Experiments with single rectangular holes in a metal confirm this result [15]. Furthermore, it is even possible to show that there is no cutoff for infinitesimal holes near the plasmonic resonance [16, 17].

2.2. Early works on meshes, grids, and hole arrays

As early as 1962, there have been works reporting transmission resonances through metal grids [4, 18, 19], meshes [19, 20], and circular hole-arrays [21, 22]. Fig. 1 shows early measurements of resonant transmission through a mesh. These were studied for their filtering capability with applications in antennas, frequency-selective surfaces, laser mirrors, solar filters and artificial dielectrics [23]. A phenomenological model for the light transmission through square apertures was provided using an inductor-capacitor circuit [18], which was extended with a resistor to include loss. An early work provided an explicit formulation for the scattering between holes using Bethe's theory, yet they did not explore the resonances for a lattice period close to the wavelength [24]. Later, a numerical evaluation of the transmission was given, showing a resonant dip in reflection that was influenced by the surrounding media [21]. Subsequently, simple analytic expressions were found for arrays

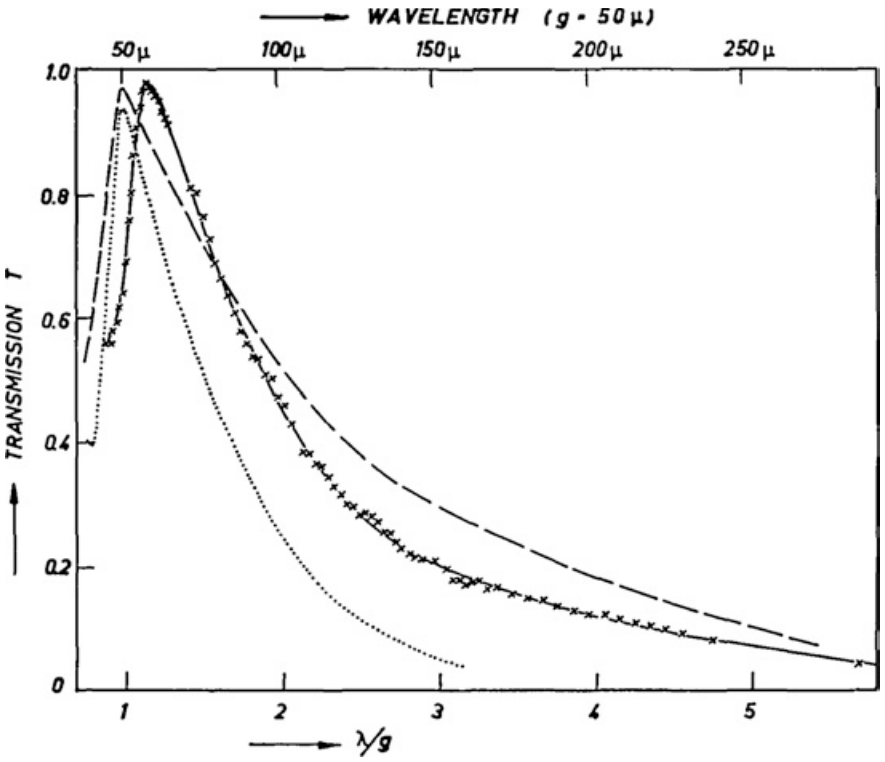

Figure 1 Measured transmission through strips (dashed and dotted lines) and two-dimensional meshes (crosses and solid line). g is the grating period and the strip width of the mesh was an eighth of the period. (Reprinted with permission from [4], © 1962 Optical Society of America)

of holes above cutoff [23]. Different hole-sizes and shapes were studied; however, the case of resonances for small apertures in the Bethe limit was not explicitly provided.

In those early works, in the absence of loss, a resonance was found with total transmission. Fig. 1 shows near-perfect transmission at the resonance with finite loss. While Bethe's theory for a single aperture suggests that the transmission will go down rapidly with the hole-size, less than total transmission at the resonance for an array of smaller holes was not predicted by that early theory. Furthermore, experimental works have explored the transition between small and larger apertures (relative to the wavelength), and found qualitatively different behavior since in the small-hole case, a single mode can be considered [25]. As we shall see in the next section, an array of subwavelength holes still gives a complete-transmission resonance when using Bethe's theory.

2.3. Bethe's theory for aperture arrays

Arrays of apertures much smaller than the wavelength allow greater transmission than predicted by Bethe's theory for a single hole. This has many potential benefits, including the ability to squeeze the optical energy into extremely small areas. In fact, Bethe's theory, when applied to arrays of holes, gives full transmission at the resonant wavelength [26, 27]. The first work to describe the transmission through aperture arrays in the Bethe limit considered the Babinet compliment to the hole-array: an array of disks. It was found that the disk-array provided zero transmission at a resonant wavelength [26]. Zero transmission results from the cumulative effect of the multiple scattering between disks, where each disk is treated as a dipole scatterer in an infinite sum over the array. By Babinet's principle, this means that an array of holes gives 100% transmission at the same wavelength. Another approach is to consider the periodic nature of the problem, which allows for a single propagating plane wave and an infinite number of evanescently bound modes at each side of the aperture array [27]. In the small-hole limit of Bethe's theory, for periodicity close to the optical wavelength, only one of the evanescent modes needs be considered because its magnetic field becomes arbitrarily large close to the cutoff. Therefore, this transverse magnetic (TM) mode dominates the coupling to the aperture that is formulated in terms of a magnetic dipole in Bethe's theory, as described above. If only this TM mode (on both sides of the film) and the incident and transmitted electric fields are considered in a self-consistent way, total transmission is found at the resonant wavelength. Fig. 2 shows the result of this self-consistent calculation for the wavelength-dependent transmission of arrays of different aperture shapes – the aperture shape influences the magnetic polarizability of Bethe's theory, and thereby, modifies the transmission resonance profile. Another feature of Fig. 2 is that the transmission goes to zero when the wavelength equals the periodicity. This phenomenon was explained by Lord Rayleigh in 1907, where he showed that an array of subwavelength apertures should give zero transmission from their mutual coupling [1]. (It is interesting to note that Lord Rayleigh's elegant explanation was to describe the anomalous absorption of gratings seen by

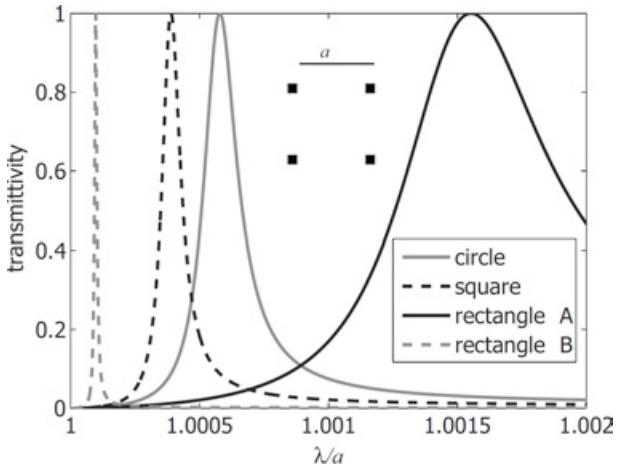

Figure 2 Transmission spectra of polarized light for a square array of holes in an infinitely thin perfect electric conductor using Bethe's theory. Different hole-shapes have different transmission spectra, yet each has the same area (2% of the total area of the screen). Rectangle A is half as wide as it is long, and rectangle B is half as long as it is wide, and in each case the width dimension is aligned with the electric field polarization. (Reprinted with permission from [27], © 2007 American Physical Society)

R. Wood and referred to as the Wood's anomaly; however, for analytic simplicity, the geometry actually described was an array of apertures.)

To summarize the physical mechanism of transmission in parts: (1) the apertures couple the incident radiation into evanescent modes on both sides of the material that are bound at the surface; (2) the energy stored at the surface builds up; (3) the stored energy is re-scattered into the transmitting mode on the other side of the screen to provide total transmission, while destructively cancelling the reflected light on the side of incidence to provide zero reflection. This effect is similar to a Fabry-Perot cavity, where 100% transmission can be obtained through two highly-reflecting mirrors because energy is stored within the mode of the cavity at resonance. An important difference is that the aperture array allows for non-resonant transmission as well; directly through the apertures, by-passing the evanescent modes. The non-resonant (direct) and the resonant (aperture-evanescent wave scattered) paths interfere to produce a Fano line-shape [28, 29]. These two paths have been seen clearly in time-domain numerical studies, where the resonant transmission is delayed with respect to the non-resonant transmission [30].

There is a simple interpretation of why only a single TM mode dominates the transmission for small holes. In the vernacular of electrical engineers, the magnitude of the admittance of the aperture increases as it is made smaller. Similarly, the TM mode's admittance magnitude (given by the ratio between the transverse magnetic and electric fields) also increases as the mode approaches cutoff. Therefore, the coupling of the aperture to the single TM mode can be thought of as impedance matching for optimal resonant energy transfer, whereas the other modes do not couple efficiently to the aperture.

The physics is complicated by the material response at different wavelengths, finite film-thickness, the hole-shape, and the lattice arrangement. The influence of each of these effects will be described in more detail in the following sections.

2.4. Real metals at different wavelengths

The transmission properties of an aperture array depend considerably on the material used and the optical wavelength. For long wavelengths (mid-infrared to microwave), metals are well-approximated as perfect conductors and near-perfect resonant transmission has been found experimentally for thin metals, which agrees well with the theoretical conclusions of the previous sections. In the visible and near-infrared regimes, the response of the metal plays an important role, and the transmission resonance is typically much less than unity.

The observation of EOT in the visible – near-infrared regime, by Ebbesen and co-workers, was suggested to arise from coupling to surface plasmons [7, 31]. Surface plasmons can be propagating surface plasmon polaritons (SPPs) or localized surface plasmons (LSP). The SPP is a TM waveguide mode that exists at the interface between a metal and a dielectric when the real permittivity of the metal is negative and its magnitude is greater than that of the dielectric. Unlike dielectric waveguide modes, SPPs require only a single interface, and the mode is exponentially bound at the surface, decaying both into the metal and towards the dielectric. The wave-vector of the SPP is given by:

$$k_{\mathrm{SPP}} = \frac{2\pi}{\lambda_0}\sqrt{\frac{\varepsilon_d \varepsilon_m}{\varepsilon_d + \varepsilon_m}} \qquad (1)$$

where λ_0 is the vacuum wavelength, and $\varepsilon_{d,m}$ is the relative permittivity of the dielectric, or metal. When $\mathrm{Re}[\varepsilon_m] < -\mathrm{Re}[\varepsilon_d]$, the SPP wave-vector is larger than the dielectric wave-vector. The Bragg-condition for resonance of the SPP with the periodicity of a rectangular array is given by:

$$k_{\mathrm{SPP}} = 2\pi\sqrt{\frac{i^2}{a^2} + \frac{j^2}{b^2}} \qquad (2)$$

where a, b are the x and y direction periodicities of the array and i, j are the whole number resonance orders along the x and y directions, respectively. These resonances are shown with solid lines in Fig. 3, along with the transmission spectra observed for holes in the square lattice of a silver film on quartz.

The SPP is an important component of the surface waves described in the previous section, and the resonant transmission occurs close to the Bragg resonance for the SPP. In addition, there can be LSPs within the holes that also play a role, as will be discussed in more detail in the next two sections. Both SPP and LSP modes can be present

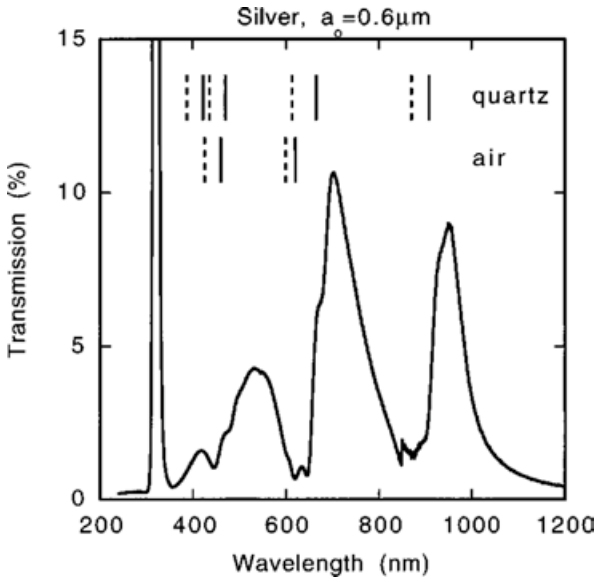

Figure 3 Transmission through a 200 nm thick silver film on quartz with 150 nm diameter square hole array, with period 600 nm. Resonances expected from SPPs shown with solid lines, and Wood's anomalies with zero transmission shown with dashed lines. (Reprinted with permission from [31], © 1998 American Physical Society)

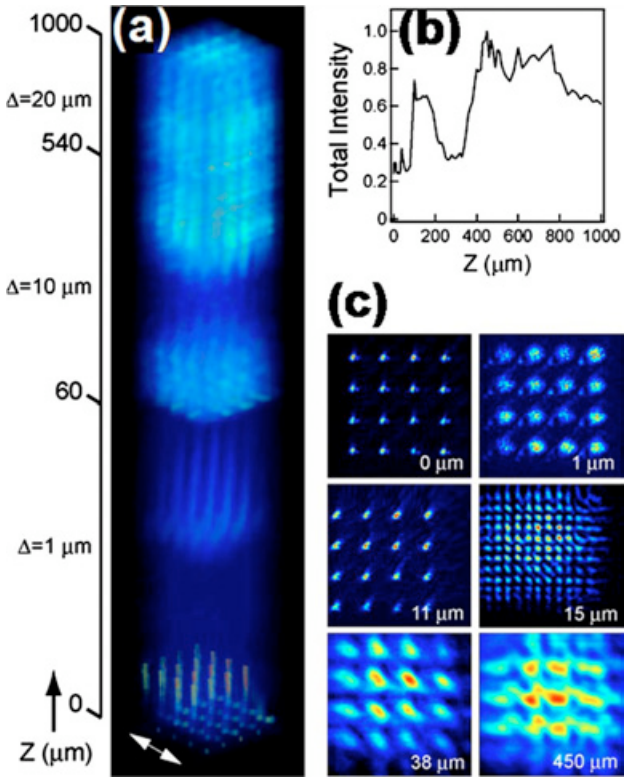

Figure 4 (online color at: www.lpr-journal.org) Three-dimensional NSOM scan above a 4 × 4 array of subwavelength holes in silver. a) Talbot-like image reconstruction. b) Total intensity scattered by NSOM tip over entire image. c) Images at different heights (self-normalized). (Reprinted with permission from [52], © 2007, American Institute of Physics)

for free-electron metals in the visible regime, and therefore, they are important for EOT at those wavelengths.

The role of SPPs on EOT has been debated vigorously in the literature [31–39]. Some works have suggested that the diffraction of many evanescent modes is required to fully-explain the transmission, and the single SPP description is not sufficient. Several works have studied the role of the SPPs in EOT. Reflection measurements showed an increase in absorption at regions of the transmission resonance [40]. Furthermore, they showed that the polarization dependence was consistent with a TM surface wave, even for angled incidence, which supports the hypothesis that SPPs play an important role at visible wavelengths. Experiments have been performed where silver was added to a nickel membrane, and it was shown that the EOT was enhanced most for the case where both surfaces were covered with silver [41], which suggests that metals with lower losses and supporting SPPs show greater EOT in the optical regime. Comparisons have been made between noble metals and transition metals, showing that noble metals, which support SPPs in the visible, have greater transmission [42]. Interestingly, aluminum was not studied in that work, but it has been studied in a recent theoretical paper [43] which showed large EOT in the visible regime where the relative permittivity has a large negative magnitude. Tungsten was studied in detail theoretically, and although it cannot support SPPs due to a positive real permittivity, it shows enhanced transmission and enhanced local field intensity at the metal surface close to the geometric resonances [44]. It was noted that similar effects are not expected in germanium due to the relatively small magnitude of the relative permittivity when compared to tungsten. Experimental studies of chromium films also showed transmission resonances in the near-infrared [45].

Near-field scanning optical microscopy (NSOM) is a useful tool to visualize surface waves and mode-distributions in the near-field with resolution below the diffraction limit. As a result, it has been used extensively to study the role of SPPs in EOT [46–52]. The scattering to surface waves by the nanohole arrays has been observed [47]. Away from the surface, the field pattern observed by NSOM was redistributed so that light emission was attributed to the region around the holes [46]. In addition, interesting diffraction effects, such as Talbot-like imaging away from the surface, have been observed as shown in Fig. 4 [52]. The Talbot effect is a self-imaging property of gratings, where there are several focal planes for a particular wavelength. Near-field experiments on hole-arrays with spacing greater than the SPP wavelength have shown interference fringes that agree well with SPP excitation, as shown in Fig. 5 [53]. A theoretical study showed that the near-field was influenced by the lattice in calculations of 20 nm silver films in the near-infrared [54].

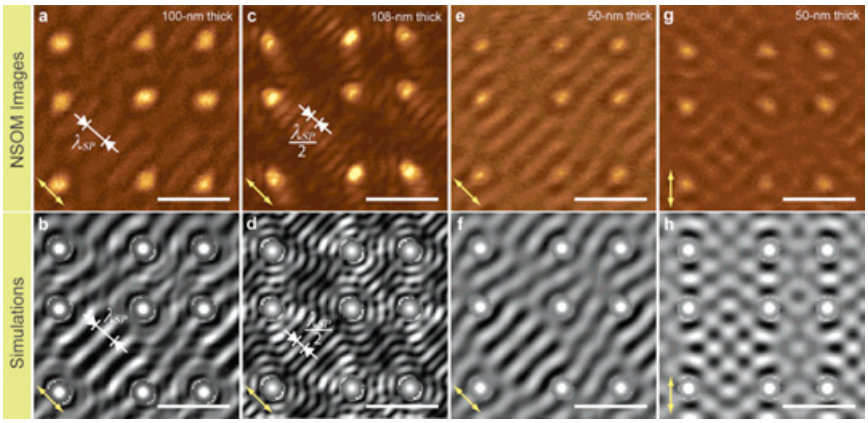

Figure 5 (online color at: www.lpr-journal.org) NSOM images of surface waves interfering above nanohole arrays fabricated in gold by photolithograpic methods, and corresponding simulations supporting the role of SPPs. (Reprinted with permission from [53], © 2006 Americal Chemical Society 2006)

There has also been substantial investigation of hole arrays in the terahertz (THz) regime. At THz frequencies, the transmission resonances are less sensitive to the type of metal used due to the large magnitude of the relative permittivity [55, 56]. Thus, there is less distinction between the metal and a perfect electric conductor [57, 58], leading to almost negligible penetration of the electromagnetic field. The metal loss, however, can play a role in the magnitude of transmission [58, 59]. In the THz regime, the EOT shows stronger transmission than in the visible, with 5 times more light transmitted than directly incident on the hole-area [55].

Other materials have also been studied in the THz regime because of the diverse material responses in that frequency range. For example, SiC possesses strong phonon-polariton resonances that are similar to surface plasmon resonances but these exist in the infrared. SiC films perforated with hole-arrays also show transmission resonances close to the array periodicity, as well as enhanced absorption [60]. Doped Si has been demonstrated to provide SPP-influenced EOT in the THz regime [61]. In addition, the THz response of InSb is strongly temperature dependent and this can be used to tune the resonance properties [62].

For millimeter waves, transmittance values higher than 0.95 have been observed [63]. Due to the high quality of the resonance, the size of the array plays an important role in the transmittance at those wavelengths. Especially as the holes are made smaller, the quality of the resonance increases, as expected from Bethe's theory applied to aperture arrays, so that a finite array has less transmission. Near-field studies have also been carried out in the microwave regime, where the phase of the electric field was also resolved [64]. That work showed clearly the dipole nature of the holes as scattering elements.

2.5. *Film thickness*

The physics of transmission through hole-arrays is dependent in a number of ways on the film thickness. For real metals, the film thickness should be at least comparable to the finite penetration depth of the electromagnetic field into the metal in order to observe significant resonances [65]. As the film thickness is increased, the hole becomes a channel and the coupling between surface waves on the two sides of the film is modified, and for thick films, it can become exponentially weaker [66]. Thicker films can also have localized resonances within the holes which come from reflection of the waveguide mode at the hole-ends [67]. Thick films modify the scattering of surface waves on one side of the film, allowing for so-called "spoof" surface-plasmons [68] even for perfect metals, and this mechanism can also be modeled to have an influence on the transmission as well.

The influence of film thickness, or equivalently hole-depth, on the transmission was studied experimentally for optically thick silver films in the near-infrared [66]. For thick films, the transmission resonance was reduced exponentially with film thickness. This was attributed to the exponential decay of the waveguide mode within the hole; essentially, light tunnels through the hole. For hole-depths less than 200 nm, the transmission maximum was less sensitive to the film thickness (for values greater than the skin depth). It was postulated from those observations that the SPPs on either side of the film are strongly coupled for film thicknesses less than 200 nm, and become less strongly coupled as the film thickness is increased. Supporting this hypothesis, the dispersion curves showed stronger band-bending for thinner films, which indicates stronger coupled-mode behavior. The influence of film thickness was studied for 0.3 THz transmission through aperture arrays in aluminum films [65]. It was found that the transmission resonance becomes stronger as the film thickness is increased, up to the skin-depth, where the metal becomes optically thick.

From a theoretical point-of-view, it is well-recognized that the lowest order waveguide mode excited inside the hole dominates the transmission process for thicker films. In comprehensive numerical investigations, it was shown that a single mode actually dominates the transmission of hole-arrays [69]. This was most clearly demonstrated by artificially reducing the excitation of each mode and noting the change in the total transmission [70]. A truncated model was used to produce an analytical theory of transmission using only a single mode within the hole [71].

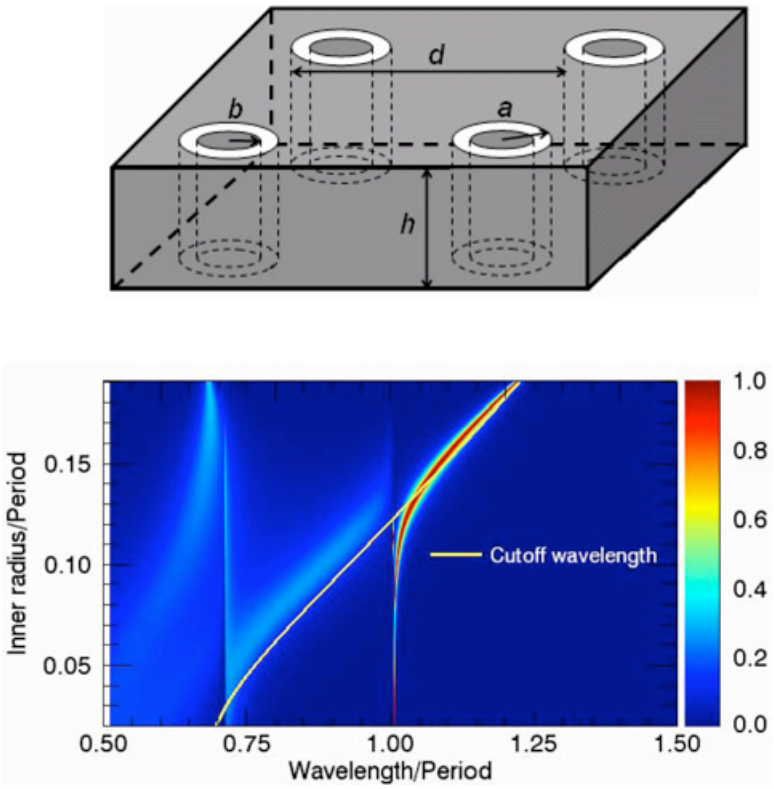

Figure 6 (online color at: www.lpr-journal.org) Transmission through an array of coaxial apertures in a perfect electric conductor (top), shows a resonant wavelength that is tuned by the cutoff wavelength of the aperture (bottom). (Reprinted with permission from [77]. © 2006 Optical Society of America)

If the hole is made larger, or shaped appropriately, it is possible for at least one waveguide mode to propagate inside the hole, instead of exponentially decaying. The transition between propagation and evanescent decay of waves inside a hole is referred to as the cutoff. For a rectangular hole in a perfect electric conductor, the cutoff of the lowest order mode occurs when the longest side is half the optical wavelength. Propagating modes inside the hole, or even for modes close to cutoff, give Fabry-Perot resonances since there is reflection from impedance and mode-shape mismatch at the ends of the hole. When the reflections between the ends of the hole add up in-phase, the field is enhanced within the hole and there is also increased transmission. The phase-of-reflection can be quite large for small holes and this is enough to allow a resonance in thin films and close to the cutoff, where there is no phase-of-propagation [67]. This effect has been described theoretically for a single rectangular hole in a perfect metal [67], and in a real metal [72, 73], and for random arrays of rectangular holes in real metals [74] and perfect electric conductors [75].

The Fabry-Perot resonances inside holes are sometimes referred to as LSPs, since they are localized at the hole and modified by the response of the metal [73]. A number of works have studied the influence of the Fabry-Perot resonances on the extraordinary transmission through hole-arrays for different hole-shapes (for example, [75–77]), and they will be discussed in detail in the next section. Fig. 6 shows clearly how the transmission resonance from a periodic array interacts with the Fabry-Perot resonance close to cutoff for co-axial hole-shapes. An experimental signature for the Fabry-Perot resonances is that they do not respond to angle-tuning, which does influence the surface-waves coupled to a periodic hole-array. As a result, the angle-tuned dispersion shows a flat-band response, which has been demonstrated for square-hole arrays in the infrared using copper meshes [78], as shown in Fig. 7.

Thick perfectly conducting films with holes can support "spoof surface plasmons" [68, 79], as mentioned earlier. These "spoof surface plasmons" arise for wavelengths larger than cutoff because the electromagnetic field decays evanescently into the hole, just like it would in a metal. The influence of this type of surface plasmon has been studied experimentally in the GHz regime [80]. For thicker films, the mode within the hole becomes important, and even and odd coupling between the surface modes on each side of the metal film is possible; this provides a double resonance in transmission with the shorter wavelength resonance coming from the out-of-phase coupling [8, 81].

2.6. Hole-shape: basis effects

In the previous section, the channel-waveguide properties of the hole were shown to influence the transmission properties. Changing the hole-shape influences not only the waveguide properties of the hole, but also the scattering to electromagnetic modes on either side of the hole. Even for infinitely thin perfect electric conductors, the magnetic polarizability and electric polarizability of the aperture are

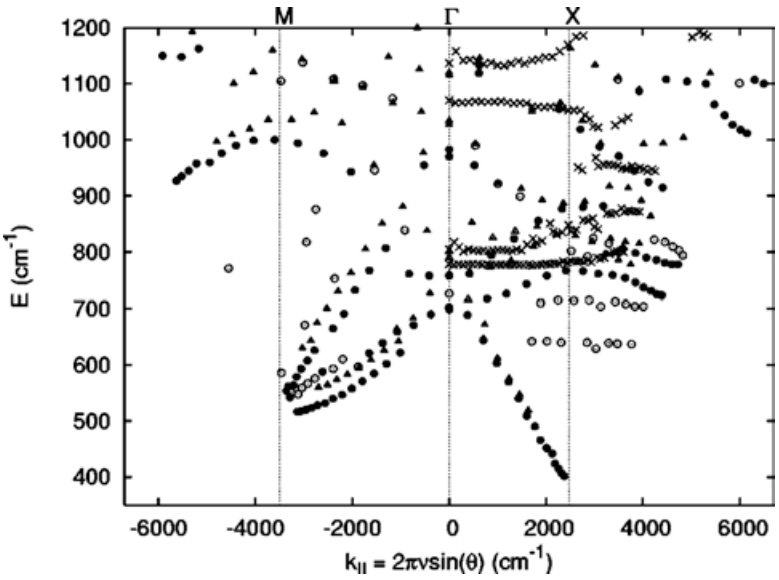

Figure 7 Angle-tuned dispersion of transmission resonances through a square-hole square-array. "x" symbols show flat-band response associated with localized Fabry-Perot resonances. (Reprinted with permission from [78], © 2004 American Institute of Physics)

influenced by the shape of the aperture. The hole-shape can also be used to modify the electromagnetic field distribution, to influence the polarization and to create resonantly excitable near-field "hot-spots". Many different hole-shapes that have been investigated including cylindrical, cylindrical coaxial, elliptical, square and rectangular, rectangular coaxial, cruciform, C- shaped, H-shaped, E-shaped, double-hole (overlapping and non-overlapping), triangular and star-shaped holes. In addition, the hole-shape has been varied along the length of the holes, for example tapered, variable radius, and screw-shaped holes.

Arrays of cylindrical coaxial, or annular, apertures have been studied at least since 1988 [82] and revisited recently. For a perfect electric conductor, there is no cutoff of the lowest-order mode of the coaxial structure; but also, due to rotational symmetry, a normally incident plane-wave does not couple to that mode, so it does not play a role in the transmission. The next lowest order mode can have a cutoff that is modified by adjusting the inner radius, and this influences the transmission, as described in the previous section. For real metals, the cutoff of the corresponding TE_{11}-like gap-mode is influenced by the metal response as well as the gap and it has been referred to as the cylindrical surface plasmon (CSP) mode [83–85]. Field intensity enhancements of 600 have been calculated inside the annular holes [86]. Compared with similar hole-arrays, the transmission can be more than doubled, and the multiplication, compared to area is ~ 8 [87]; however, those are only example calculations and the enhancements depend on the precise structure considered. Experimental works have been carried out on annular aperture arrays in the visible [88] and infrared [89, 90].In the infrared, the light transmission was found to be doubled for a coaxial hole when compared to circular apertures of the same size. Rectangular coaxial guides in real metals also have a gap surface plasmon mode, which was found to dominate the resonant transmission in numerical studies [91].

Anisotropic hole-shapes, such as elliptical [92] and rectangular [93–97] holes, show a strong polarization dependence of transmission. A single rectangular hole is influenced strongly by the aspect-ratio; the cutoff actually increases by narrowing the hole and this leads to a red-shift in the LSP resonance [14, 72, 73]. The scaling of the ratio of polarization to the aspect-ratio for elliptical holes has been treated theoretically using a quasistatic approach [98]. Elliptical holes with alternating orientation allowed for THz polarization control of the peak resonance wavelength and amplitude with varying polarization angle [99]. A comparison between the shape effect for rectangular, elliptical and circular holes has also been explored experimentally within the THz regime [56, 100].

As well as influencing the waveguide polarization properties, anisotropic hole-shapes also influence coupling to surface waves. As a result, the orientation of the hole-shape with respect to the lattice plays a role in determining the relative excitation of each resonance [92, 101, 102]. Recent NSOM studies have confirmed the result that elliptical holes scatter predominantly into TM surface waves perpendicular to the major axis [51]. For elliptical holes and rectangular holes, both the waveguide and surface-wave coupling are polarization dependent; however, for non-overlapping double-holes, the waveguide modes are nearly-isotropic so that the polarization influence of surface-wave coupling is the only remaining polarization mechanism [101].

Arrays of cruciform, or cross-shaped, apertures have been consider for the transmission resonance properties as early as 1983 [103]. Similar to rectangular holes, cross-shaped holes have shown even greater resonance enhancements for similar hole-area, but without the polarization dependence [104]. Cross-shaped holes also allow for changing the polarization properties along both directions by varying the different arms of the cross [105]. The different responses of circle and cross aperture arrays due to their shape-dependent local resonances were compared re-

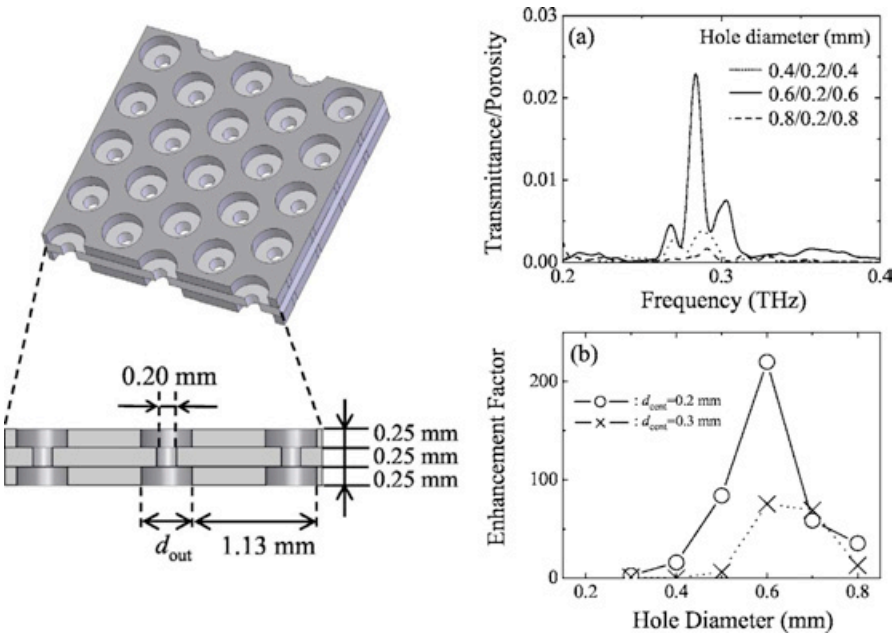

Figure 8 (left) Schematic of small-hole array clad with two big-hole arrays to enhance transmission in the sub-THz. (right) a) Transmission for various hole diameters and enhancement factor of transmission with respect to a small-hole array without outer arrays. (Reprinted with permission from [116], © 2004 American Physical Society)

cently in infrared experiments [106] (as well as for stacked aperture arrays).

Hole-shapes that lack inversion-symmetry, such as triangles [107] and three-point stars [108], are interesting for second harmonic generation, as will be described in Sect. 3.3. A triangular aperture was compared with circular and square apertures, showing enhanced linear transmission for a similar area, which was attributed to increased side-length [109].

A number of hole-shapes have been considered for their ability to reduce the effective mode area; including H-shape, C-shape and E-shape apertures. In these apertures, the electric field is concentrated inside the narrow gap region [110–112]. Experimental comparisons between C, E and rectangular hole-shapes have been performed in the THz regime [111].

In a similar fashion to the H-shaped hole, the overlapping double-hole provides a narrow gap where the field is strongly confined. An advantage of the overlapping double-hole is that it allows for sharp features to be created with a blunt nanofabrication tool [113]. In the double-hole structure, as the holes approach one another, they overlap to produce two apexes, which focus light to an extreme sub-wavelength region near the tip [114]. The linear transmission properties of the double-hole depend strongly on the proximity of the apexes, and they vary significantly with center-to-center hole-spacing. The strong field enhancement in the double-hole structure also has uses for nonlinear optics and surface-enhanced Raman scattering, as will be described in Sects. 3.3 and 3.6.

It is also possible to change the hole-shape along the length of the hole to shift the resonance, enhance the transmission, or rotate the polarization. Tapering the holes in the middle has also been shown in simulations to change the transmission resonance in the infrared [115]; the taper blue-shifts and narrows the peak resonance. Similar to the taper structure, in the sub-THz region, the transmission of a small-hole array is enhanced if it is clad on either side with a large-hole array [116]. Fig. 8 shows the light transmission for this structure, reported to be over 200 times enhanced relative to a small-hole array without outer arrays. Screw shaped holes have been used to rotate the axis of polarization and induce ellipticity on a linearly polarized incident beam in the sub-THz regime [117].

2.7. Lattice effects

The arrangement of an aperture array in a metal film influences the transmission properties by modifying the coupling to surface waves. For periodic arrays, the directional axes define the direction for which surface waves are excited. As noted in the previous section, it is possible to change the orientation of the basis (hole-shape) to influence the coupling to the surface waves along the different lattice directions [101]. Other works have compared the relative influence of lattice effects (denoted SPP) and basis effects (denoted LSP) by similar methods of changing the basis shape and orientation [102]. In that work, it was suggested that the lattice effects are more important; however, the basis does play a role in how the lattice resonances are excited [101]. As an example, biaxial arrays have shown different resonances along different directions of polarization [118]. When symmetry is broken, either with the basis or the lattice, the scattering to surface waves is polarized and the transmission is polarized. Even for square lattices with cylindrical holes, the scattering of surface waves at the apertures produces depolarization [119–121]. Other studies have shown the preservation of orbital angular momentum of the resonant transmission [122].

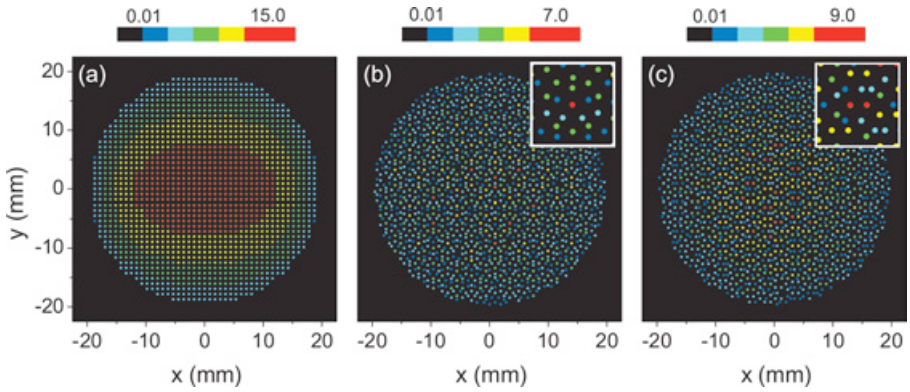

Figure 9 (online color at: www.lpr-journal.org) Calculated transmission through hole-arrays for a) finite square array and b,c) Penrose tiling array for two different wavelengths showing localized field enhancements. (Reprinted with permission from [131], © 2007 American Physical Society)

To study the scattering to surface waves, reduced arrays have been considered. For example, linear arrays of holes have been studied, as a simpler element that still has the resonances of a 2-D array [123]. As 1-D strips are added side-by-side, a shift in the overall resonance is observed due to coupling between the strips. Dark-field studies of scattering from linear arrays have shown scattering dependence on polarization and on coupling angle [124]. That work reinforces that each hole can be treated as a scattering dipole. Of particular interest, that work also shows resonances from scattering elements for distances that are much shorter than the wavelength due to the coupling of local resonances at the holes. The emission distribution is strongly angle-dependent for finite arrays, which can be interpreted as coming from the transmission of an infinite array added to the waves launched at the edges of the array from truncation [125]. As expected, for triangular arrays, the resonances follow the lattice directions once again, and in the sub-THz region, a linear increase in the transmission was observed with the number of holes for a triangular lattice [126].

Lattices with aperiodic order are interesting because they do not possess translational symmetry, yet they allow for higher-order rotational symmetry. An example of a Penrose lattice is shown in Fig. 9b. The Fourier-components of a Penrose tiling reveals its structure factor, and this has associated resonance in transmission for Penrose tiling lattices [127]. In that work, the resonances showed a shorter range behavior, saturating in normalized intensity for an array with only 200 holes, whereas similar periodic square arrays saturated at 800 holes with a linear dependence on side of the array. In another work, the comparison between an aperiodic structure (with 6-fold rotational symmetry) and periodic lattices showed greater transmission for the aperiodic structure [128], which was attributed to enhanced routes for constructive interference in the aperiodic structure. Transmission resonances have also been observed for quasi-periodic and aperiodic arrays in the THz regime, showing similar results [129, 130]. It is interesting to note that the resonances in quasiperiodic structures are localized by the array; a theoretical model of a quasi-periodic array shows the emergence of local hot-spots at individual holes that depend on the wavelength of excitation [131], as shown in Fig. 9b and c. Recent visible near-field studies of quasi-periodic structures have revealed focus spots at a significant distance away from the surface (5 μm) with widths less than half the optical wavelength [132]. Fractal aperture patterns in metal films have been investigated for their ability to show resonances over a broader wavelength range due to their self-similar structure [133].

2.8. Summary

Significant progress has been made over the past decade towards a better understanding of light transmission through hole arrays in metal films. Various configurations have been considered, both theoretically and experimentally, and we have a better understanding of the effects on transmission that arise from the real metal properties, the hole size and shape, the metal thickness, and the array periodicity. Experiments have been carried out over a wide range of the electromagnetic spectrum, ranging from visible to GHz frequencies. These investigations also point to areas of opportunity for creating hole arrays with interesting properties; for example, by exploring new hole-shapes, periodic arrangements, or materials. Based on past work, we can design hole-arrays for different applications at different wavelengths; for example, to enhance local fields or to provide efficient filtering with polarization dependence. In the next section, the applications of hole-arrays that have been investigated will be reviewed.

3. Applications

3.1. Polarization control

As described above, the polarization of resonant transmission through nanohole arrays can be controlled by the hole-shape and by the lattice arrangement. The shape-effect of the elliptical and rectangular holes can be used to produce nanopolarizers with a strong polarization dependence of the resonant transmission [92, 93]. The transmitted polarization is also influenced by the lattice arrangement because the surface waves are scattered at the hole in the direction of the electric field of the incident plane wave [101].

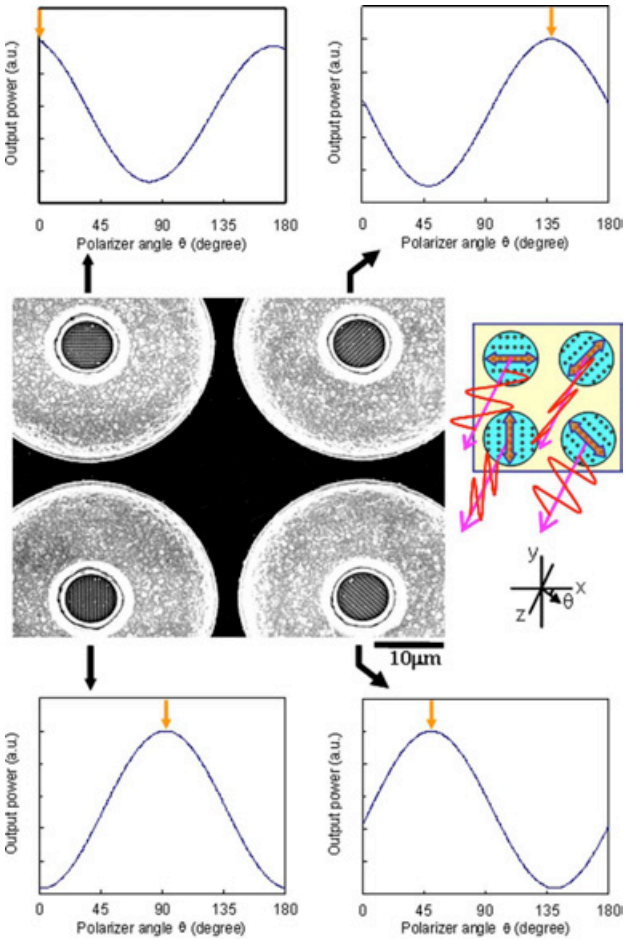

Figure 10 (online color at: www.lpr-journal.org) Polarization control of an integrated chip of four VCSELs by means of biaxial arrays of different orientation, device image and measured output polarization. (Reprinted with permission from [134], © 2007 IEEE)

Nanohole arrays on top of vertical-cavity surface-emitting lasers (VCSELs – a semiconductor microcavity laser) have been used to control the polarization of emission [134]. VCSELs are typically unpolarized, which is a disadvantage for applications where polarization stability is required. By using biaxial arrays, where one polarization is resonant and the orthogonal polarization is not, it is possible to control the output polarization state to be along one of the array's basis vectors. With careful design, it is possible to have increased transmission and reflection of one polarization with respect to the orthogonal polarization. So far, output powers of 2 mW have been obtained, which is comparable to other VCSELs. Furthermore, polarization control was obtained from 2×2 integrated VCSELs, as shown in Fig. 10.

The lattice arrangement can also be altered for polarization analysis and routing. This has been exploited for the interesting case of quasicrystals because they can possess high-order rotational symmetry. In particular, the diffraction pattern of light transmitted through a quasicrystal array is aligned along the direction of polarization [135]. Therefore, the quasicrystal can be used to determine the linear polarization by observing the orientation of the diffraction pattern and, in principle, any polarization state by using phase-sensitive interference between the diffraction spots.

It is also possible to create chiral symmetry with the hole-shape or lattice to rotate the polarization or introduce ellipticity to a linearly-polarized beam. For example, screw-shaped holes have been used to rotate the axis of polarization and induce ellipticity on a linearly polarized incident beam in the sub-THz regime [117].

3.2. Filtering and switching

The filtering effect of aperture arrays in a metal film has been considered for solar absorbers for many years and, more recently, for thermal emitters. For solar absorbers, the aperture array allows the short-wavelength visible wavelengths of the sun to pass through and be absorbed by a material behind the array. The absorbing material heats up, but it cannot lose energy by black-body radiation because the long-wavelength infrared light is reflected by the aperture array [18, 136, 137]. Most of those works considered large apertures, to pass the greatest visible light, and resonant transmission was not exploited.

For thermal emitters, the resonant transmission can be tuned to pass a narrow-band of interest from a heated blackbody. The emitted infrared radiation has a narrower-band and is directional. A subwavelength hole array was used to filter the blackbody emission of silicon structures coated with metal [138, 139]. In another work, the emission from a thin (100–500 nm) heated SiO_2 layer sandwiched between two 100 nm silver films, one with a periodic array of subwavelength apertures, showed a narrow peak of 480 nm FWHM at around 4 μm [140].

In 1962, it was demonstrated that a pair of grids in parallel could be used as mirrors of a Fabry-Perot interference filter for the infrared [4]. The results from that initial demonstration are shown in Fig. 11. Nanohole arrays in metal films have been considered for color filtering in the visible, for applications such as displays. Fig. 12 shows an example of visible filtering [9]. Polarization control of shape resonances is a way to tune the resonances of these arrays [141]. In that work, rectangular apertures were used to apply strong polarization dependence to the resonances, and two arrays with perpendicular apertures were superimposed to provide two different polarization addressable resonances. It is also possible to tune the refractive index of the material by using liquid crystals. For example, tunable optical filters have been demonstrated in the sub-THz regime by using magnetically-tuned nematic liquid crystals to change the surface refractive index and thereby change the transmission resonance wavelength of the array from 0.188 THz to 0.193 THz [142]. In that demonstration, the tuning range was significantly smaller than the

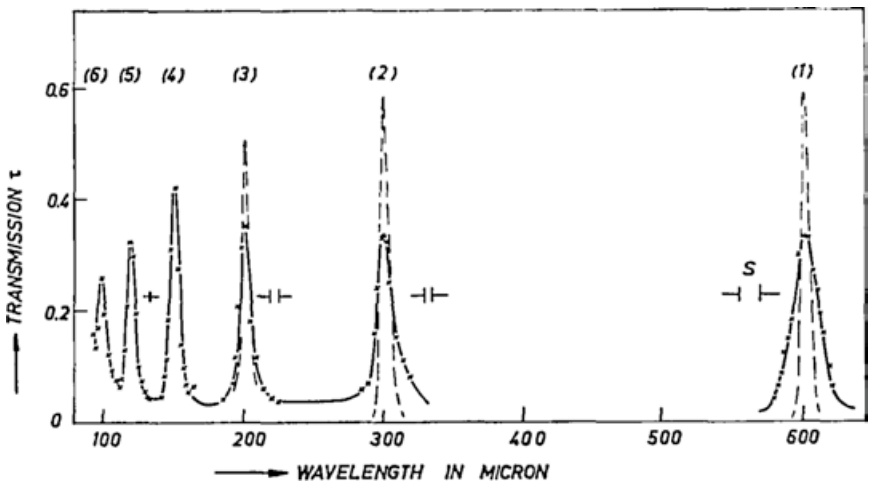

Figure 11 Fabry-Perot intereference from transmission through two grids (with 50 micron period, 12 micron strip width) spaced by 300 microns. Resolution corrected to the spectrometer slit is shown with dashed lines. Maximum finesse of 60 demonstrated with 60% transmission. (Reprinted with permission from [4], © 1962 Optical Society of America)

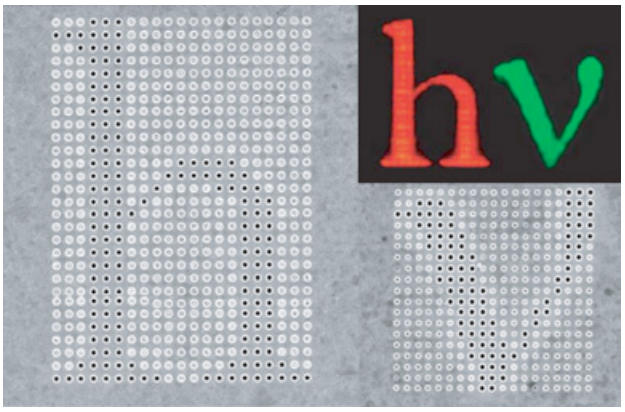

Figure 12 (online color at: www.lpr-journal.org) 550 nm and 450 nm period hole-arrays in shapes of "h" and "ν", with surrounding dimples to demonstrate red and green enhanced transmission. (Reprinted with permission from [9], © 2007 Nature Publishing Group)

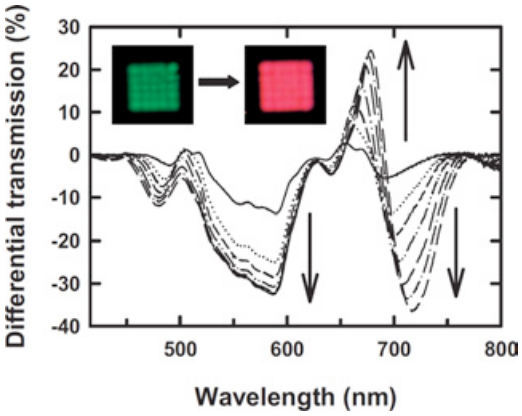

Figure 13 (online color at: www.lpr-journal.org) Differential transmission of an array of nanoholes covered with dye-doped PMMA shows changes under UV illumination (arrows indicate increased exposure). (Reprinted with permission from [149], © 2006 Wiley-VCH)

linewidth of around 0.02 THz. Theoretical works have predicted strong tuning from cylindrical holes in periodic and random arrangements when infiltrated with nematic liquid crystals [143]. It has also been proposed that magnetic fields could be used to tune the transmission properties of a hole array by influencing the Drude-Lorentz response of the medium [144, 145]. In those works, a tuning capability was predicted to be apparent for highly-doped semiconductors.

DC studies of THz transmission of hole arrays in InSb at room temperature and at 240 K showed reduced transmission with increased photogenerated (780 nm excitation wavelength) carriers [146]. Fast optical switching, between 10 ps and 100 ps, of THz waves has been obtained using a Si substrate and an optical pump pulse [147]. The optical pump generates photocarriers that turn the Si into a conductor and effectively fill in the holes with a "metal" for the THz waves.

In the visible regime, switching was demonstrated by electrically biasing liquid crystals in the vicinity of the hole-arrays, and thereby modifying the transmission at a particular wavelength at switching frequencies around 100 Hz [148]. For optically-triggered switching, monolayers of optically active materials can be used to modify the resonances, both by refractive index shifts and absorption changes to the molecule [149], as shown in Fig. 13. In that work, a photoisomer was used to obtain changes in the transmission profile, which limits the ultimate switching speed due to the rate of photoisomerization.

3.3. Nonlinear optics

The nonlinear optical response of materials is typically weak, so intense local fields and phase-matching are required to have efficient nonlinear optical conversion. Subwavelength aperture arrays in metal films are appealing for nonlinear optics research because they provide resonant enhancement of the optical field in subwavelength dimensions,

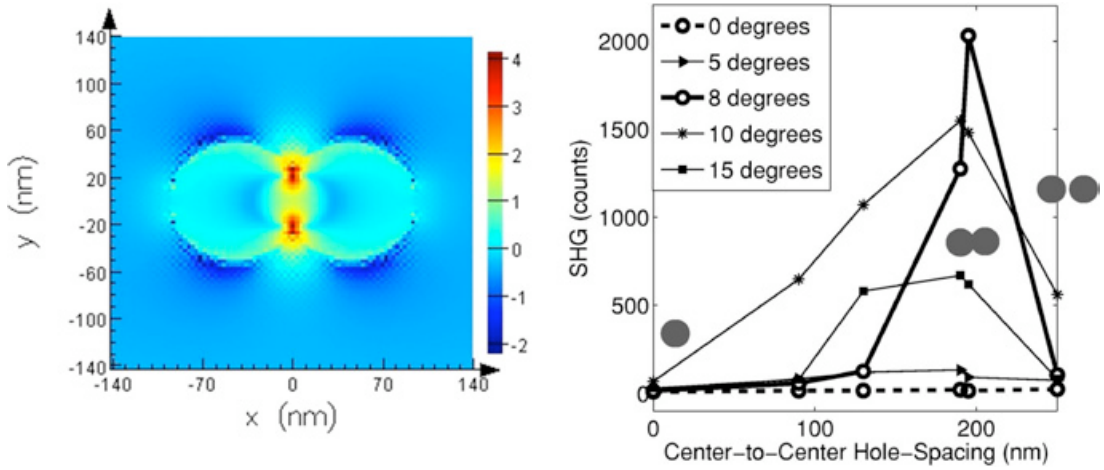

Figure 14 (online color at: www.lpr-journal.org) (left) Log-scale of field intensity enhancement in double-hole structure in gold film calculated by the finite-difference time-domain method. (right) SHG from periodic arrays of 200 nm diameter double-holes for changes in center-to-center hole spacing for various angles of sample. The maximum SHG is observed for the sharpest apex double-hole structure. (Reprinted with permission from [151], © 2007 American Physical Society)

well-below the diffraction limit. In addition, the different resonances and symmetries associated with the aperture-shape and the lattice arrangement provide opportunity for resonances and phase-matching. So far, the nonlinear optical studies have been limited mainly to second harmonic generation (SHG).

SHG studies have been carried out for periodic and random arrays. It was found that SHG in transmission was enhanced for the angle that maximized transmission of the fundamental beam, except for small angles where local symmetry forbids SHG to first order [107]. In a local dipole theory, SHG is forbidden for centro-symmetric materials and structures. Even though the maximum transmission was 5 times greater for periodic arrays, random arrays showed greater SHG for larger angles and smaller angles, because of symmetry breaking and local resonances allowed by the random lattice [107]. Also, triangular holes showed greater SHG due to symmetry breaking of the aperture-shape [107]. Symmetry breaking was further considered from asymmetric apertures and quasiperiodic lattices, which both allow for SHG even at normal incidence [108]. Furthermore, quasi-periodic lattices provided greater SHG when compared with random arrays because of their inherent long-range order [108].

Aperture shape can also allow for strong local-field enhancement, well-below the diffraction limit. Of particular interest are sharp tapers, since the surface plasmon is strongly confined as it travels to the tip of the taper. SHG from double-holes showed a pronounced increase when the double-holes were just touching to produce two sharp apexes [150, 151], as shown in Fig. 14. Due to symmetry, once again, those studies required angled incidence to obtain significant signal. Measurements using the reflection geometry showed similar results. A modified double-hole structure, where one of the apexes is milled away, has recently been demonstrated to break the centro-symmetry [152], as was done with triangular holes [107] and stars [108]. That work showed pronounced increase in the SHG for small angles [152].

Enhanced nonlinear conversion can be obtained by tuning the lattice and local resonances of the apertures individually. As described in Sects. 2.5 and 2.6, by tuning the hole-shape to cutoff, there can be an LSP from the Fabry-Perot mode inside the hole. This leads to enhanced SHG when the cutoff is tuned to be resonant with the fundamental [153]. Fig. 15 shows a strong enhancement in the SHG as the aspect ratio of the holes is varied toward the

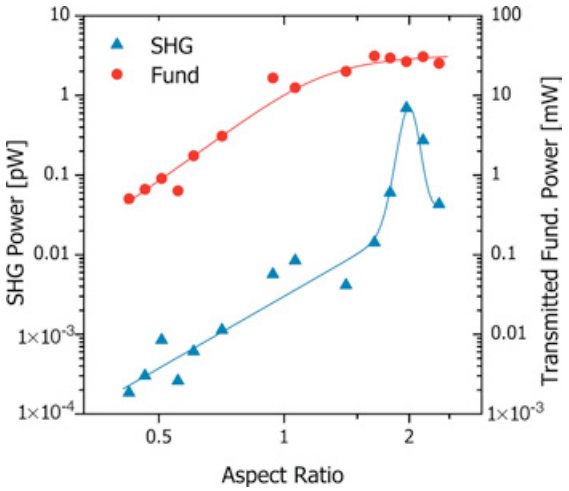

Figure 15 (online color at: www.lpr-journal.org) Dramatic increase in SHG single for arrays of rectangular holes when the aspect ratio of the rectangular hole is tuned to allow for LSP resonance, while the fundamental beam transmission only increases moderately. (Reprinted with permission from [153], © 2006 American Physical Society)

cutoff. Similar shape-resonances were observed from the sunglass structures [152], where symmetry breaking was further used to enhance SHG.

The hole-arrays can be used to enhance SHG from nonlinear optical materials inside or adjacent to the holes, as has been done for GaAs in annular apertures [154]. In that case, the resonance was associated with the LSP of the individual hole, not the lattice periodicity (for both the second harmonic and fundamental).

3.4. Surface plasmon resonance sensing

The dependence of resonance wavelength on the refractive index of the dielectric environment was recognized in early works on transmission gratings [21]. In the context of nanohole arrays in metal films, the sensitivity of the transmission properties at resonance to the refractive index of a liquid cladding the array was first demonstrated in [155]. In that work, the transmission resonance wavelength associated with the surface plasmon resonance (SPR) red-shifted as the refractive index of the liquid surrounding the arrays increased. These results are expected considering the approximation of the SPR condition for grating coupling given by Eq. (2).

The specific dependence of EOT resonances on the refractive index near-surface suggests that nanohole arrays are good platforms for chemical sensing [9]. In fact, SPR from planar gold films are well-established as an analytical method, widely used in chemistry, biochemistry and biomedicine [156]. Standard SPR biosensing is realized by immobilizing a target and monitoring the changes in the resonance upon adsorption of the molecule of interest to the target. Other assay modalities, such as competitive binding and sandwich testing, are also possible. SPR from planar gold film is usually implemented using prism coupling, which requires a total internal reflection (attenuated total reflection, or ATR) arrangement proposed by Kretschmann and Raether [157]. A typical sensitivity of prism coupling SPR systems is in the range between 3100 to 8000 nm/RIU (RIU = refractive index unit) [158]. Imaging SPR has also been implemented using the reflection configuration, allowing the multiplexing detection of several biological markers simultaneously [159, 160]. However, the reflection geometry introduces distortions to the imaging and this arrangement is not easily miniaturized or integrated in lab-on-chip devices. Arrays of nanoholes provide a series of potential advantages over the most common current SPR technology [161], and the normal transmission geometry (as opposed to the ATR geometry) is favorable for device integration [162].

The dependence of SPR from nanoholes arrays in gold films to surface adsorption events is illustrated in Fig. 16 [163]. The white light transmission through a bare array of nanoholes on gold presented a main SPR peak at 645 nm. The same array, but modified by a monolayer of mercaptoundecanoic acid (MUA) showed a 5 nm red-shift

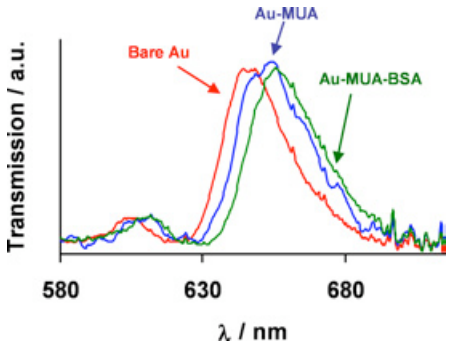

Figure 16 (online color at: www.lpr-journal.org) EOT for SPR sensing. The transmission resonance peak shifts with the surface absorption of a monolayer of MUA and again with the addition of the BSA protein. (Reprinted with permission from [163], © 2004 American Chemical Society)

in the SPR wavelength due to the changes in the dielectric properties at the surface. The adsorption of a protein (bovine serum albumin - BSA) on top of the MUA layer led to an additional 4 nm red shift in the SPR wavelength. The spectral characteristic of a bare gold surface was recovered after the surface species were removed by a plasma cleaning treatment [163]. The sensitivity obtained from this early demonstration was calculated as 400 nm/RIU, which is smaller than observed for the typical fixed-angle SPR under the Kretschmann configuration [158]. Other nanohole platforms, for instance the quasi 3-D structures prepared by a combination of nanoimprint followed by metal deposition reported in [164], have yielded better sensitivity for SPR based sensing, between 700–800 nm/RIU.

The smaller sensor output sensitivity of nanohole arrays had been tackled by improving either the instrumentation or the detection scheme [165, 166], or by the optimization of the hole-shape to take advantage of LSP resonances [167]. An example of the instrument optimization approach is the implementation of a detection scheme involving crossed-polarizers [165]. In that case, sharper, more-symmetric, transmission resonances were obtained because the crossed polarizers isolate scattered surface-mediated transmission from the unwanted direct transmission [165, 168, 169]. Sensitivities approaching conventional SPR have been reported using that approach. The concept of enhanced sensitivity by hole-shape optimization was demonstrated by using a double-hole basis to follow the real-time adsorption of BSA [167]. The role of the localized surface plasmon modes at the apexes of the touching double-hole structure in the enhanced sensitivity was confirmed by finite-difference time-domain calculations. An alternative to these efforts to improve the device sensitivity is to devise analytical methodologies that increase the response to the binding event. A common example is the application of sandwich assays in SPR [170]. The detection antibody can be even tethered to a gold nanoparticle which will introduce a 3-fold enhancement in the sensitivity of protein detection using nanohole arrays [171].

As an alternative to wavelength-shift detection, it is possible to monitor the extent of adsorption by measuring intensity variations in a transmitted monochromatic beam [172]. The wavelength of the transmitted light must be within the SPR peak. The steepest edge of the transmission band should provide the best sensitivity. A limitation of this approach is the changes in intensity from spurious effects, such as scattering by particles in the solvent, which cannot be separated from the signal changes. Biaxial arrays with different resonance peaks for the two orthogonal polarizations were introduced to overcome this limitation [173]. The shift in SPR due to molecular adsorption led to an increase in the transmission for one polarization and a decrease to the other. The spurious intensity variation can be eliminated by analyzing the adsorbate-induced changes in relative intensity from both polarizations.

Due to their small size, nanohole arrays offer the possibility of reduced detection limits, since the signal originates from a small area. Limit of detection in the attomolar (10^{-18} Mol) range has been recently reported for SPR using arrays of nanoholes [174]. The approach consisted in blocking the top surface area of the array with a dielectric layer (SiO_x), limiting the detection to the gold surface inside the holes. Surprisingly, the blocking of the top surface did not decrease the sensor output sensitivity of the array, indicating that the LSP mode inside the hole plays a dominant role in this case. Each 170 nm diameter hole can accommodate an estimated 2000 proteins in its inner surface for an array of 900 holes that was used. This areal limit of detection can be further decreased by taking advantage of smaller arrays without affecting the output sensitivity of the device [175]. The in-hole detection of proteins adsorbed on surface immobilized phospholipids at the bottom of nanoholes in random arrays has also been demonstrated [176]. In that case, the gold surface was blocked by the non-specific adsorption of BSA. The same approach was implemented for cancer biomarker detection, with an estimated limit of detection of 0.1 pg of the antigens per mm^2 [177].

The application of nanohole arrays in chemical sensing to date have only explored the plasmonic properties of these structures. However, these arrays are fundamentally channels that could be harnessed for analyte transport under a nanofluidics regime. The concept of a flow-through chemical sensor based on nanohole arrays that take advantage of both plasmonics and fluidics properties of this platform, has been suggested in [12] and demonstrated recently [178]. The final objective is to have the gold surface coated with a dielectric material and the sensing area will be confined to the inside of the holes [174]. The analyte diffusion to the inside walls of the nanoholes will be greatly accelerated by this approach due to the reduced cross-sectional area; rapid transport is enabled by the nanoscopic dimensions of the channels. More importantly, the flow-through scheme confines the analyte to the same region of the concentrated electromagnetic field, for inherent sensitivity.

Although most of the efforts on the application of nanohole arrays as chemical sensors are centered in self-assembled monolayers and biological systems, the EOT phenomenon can also be used to monitor dielectric film thickness. Experiments in the infrared allow the detection of films up to 200 µm [179]. The transmission properties in those experiments were different when just the input side of the nanoholes was coated compared to when both (input and output sides) were coated. A lower sensitivity was observed for the asymmetric arrangement, suggesting that a through-film surface-wave interaction is required in that regime. Ni meshes have also been used to determine the thicknesses of TiO_2 films in the middle IR [180].

3.5. Surface-enhanced fluorescence

Fluorescence spectroscopy is used widely in the detection of biological species. Although most fluorescence-based assays are not "label-free" (in contrast to SPR), they present higher sensitivity and their detection limit can reach the single-molecule level [181]. The concept of plasmonic structures enhancing fluorescence might seem contradictory at first glance, due to the well known quenching of emissions from adsorbates on metal surfaces [182]. However, while the quenching mechanism is short-range and only important for species in immediate contact to the metal, the surface plasmon field extends several nanometers away from the surface, providing enough field strength to increase the emissions for species located more than 5 nm away from the surface and within the surface plasmon field [183].

Initial experiments of enhanced fluorescence from species adsorbed in nanohole arrays used a monochromatic light source and measured the dependence of the fluorescence intensity on the angle of incidence of the excitation. The SPR conditions led to a 40 times increase in the fluorescence emissions [184]. This level of enhancement was confirmed in normal transmission experiments, where the excitation energy was transmitted through the nanoholes and excited a dye immobilized in a polymeric matrix in contact to the gold surface [185]. Fig. 17 shows the dependence of the measured enhancement factor (EF) with the periodicity of the array. Since the geometry of the experiment was

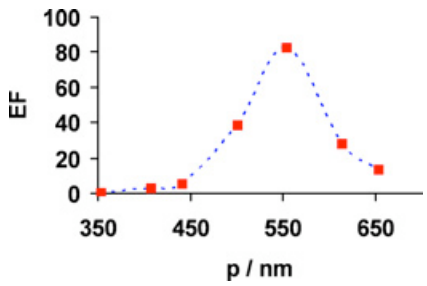

Figure 17 (online color at: www.lpr-journal.org) Enhancement factor (EF) of fluorescence observed for nanohole arrays of varying periodicity (p). The maximum fluorescence corresponds to the maximum in transmission. (Reprinted with permission from [185], © 2005 American Chemical Society 2005)

kept constant, the array that allowed maximum transmission of the exciting field at normal incidence presented the largest EF.

Affinity assays were devised to take advantage of the enhanced fluorescence enabled by nanoholes [186]. The nanohole platform offers a nanoscopic region for analyte confinement inside the holes. The surface plasmon modes inside the holes also lead to enhanced fluorescence [187]. The in-hole enhancement is mainly due to LSP modes [188], but other factors, such as increased light collection efficiency, contribute to the observed enhancement. Antibodies can be specifically placed in the nanoholes using a nanopipet, generating high density arrays for simultaneous fluorescence read-out [189].

Nanoholes are also suitable as zero-order waveguide platforms for single molecule fluorescence, where all modes inside the holes are cutoff [190]. In this case, the effective probed volume is given by the field distribution inside the hole and the dynamics at the molecular level can be followed by monitoring a single molecule diffusing in and out of the field. For instance, a 6.5 increase in the fluorescence emission from single molecules was reported from a single hole in aluminum [191].

The fluorescence enhancement is generally accompanied by a lifetime reduction due to the quenching effects and the direct transfer of energy from the molecular excited state to surface plasmon modes at the metal. A notorious exception was the moderate reduction in the lifetime observed for Rhodamine 700 on hole arrays; however, in that case, a spacer layer was used, so there was likely no infiltration of the dye into the holes [192].

3.6. *Surface-enhanced Raman scattering*

Normal Raman scattering is a weak effect, but the Raman signal can be significantly enhanced for molecules adsorbed at plasmonic structures in surface enhanced Raman scattering (SERS) [193]. The Raman scattering from a molecule at a metal nanostructure is enhanced by the surface plasmon local electric field at the laser excitation frequency. The Stokes-shifted scattered photons from the molecules are generally within the surface plasmon envelope, since the bandwidth of the SPR from nanostructures is much larger than the molecular vibrational energy. The Raman scattered photons from the molecules can then also excite surface plasmons, providing an additional enhanced field at the Raman-shifted frequency. As a result, the SERS intensity will scale as the fourth power of the local field enhancement. The role of surface plasmons in SERS is now well-accepted and this effect has been observed for species adsorbed at different plasmonic platforms, including random [194] and organized structures [195]. Nanohole arrays are interesting for SERS investigation because they allow for resonantly-enhanced local fields at the surface of the nanostructured metal film.

Fig. 18 shows the SERS results from a probe molecule, oxazine 720, adsorbed on arrays of nanoholes in gold films [196]. In the forward scattering experimental geometry, the laser beam is transmitted through the nanoholes to excite the species adsorbed at the opposite gold surface. Experiments using arrays with different periodicities showed a relationship between the SERS intensity and the EOT at the laser excitation. The strongest SERS is observed for the array that provides the best match between the laser excitation and the EOT peak.

The estimated SERS EF for the probe molecule, oxazine 720, relative to the normal Raman of liquid benzene was 10^5 [196]. Oxazine 720, however, has an electronic absorption that coincides with the wavelength of the excitation laser. This means that the experimental EF contains extra contributions from the resonance Raman (RR) effect. Typically the EF due to the RR is between 10 and 10^2. Experiments using molecules that do not support RR at the laser excitation, such as rhodamine 6G dye and pyridine, adsorbed on nanohole arrays in gold did not show any measurable SERS in the initial studies on cylindrical holes. SERS spectra from oxazine 720 adsorbed on nanohole arrays in copper with different periodicities were also obtained [197]. Although the relative EF obtained for copper was an order of magnitude smaller than for gold, a similar relationship between the SERS efficiency and the periodicity of the arrays was observed. The maximum SERS was observed for the array periodicity that provided the largest local light field strength at the excitation wavelength, as determined by numerical simulations. A quantitative eval-

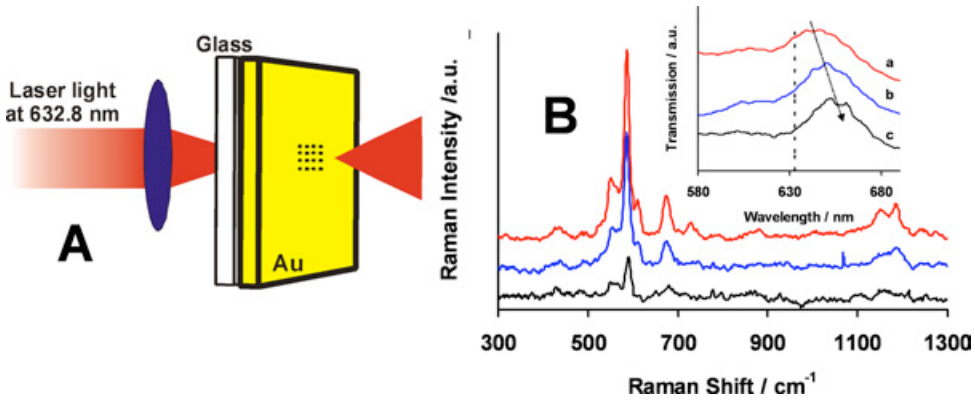

Figure 18 (online color at: www.lpr-journal.org) (A) Transmission geometry for SERS measurements. (B) Enhancement of Raman signal observed for arrays with greater white light transmission (inset). (Reprinted with permission from [196], © 2005 American Chemical Society)

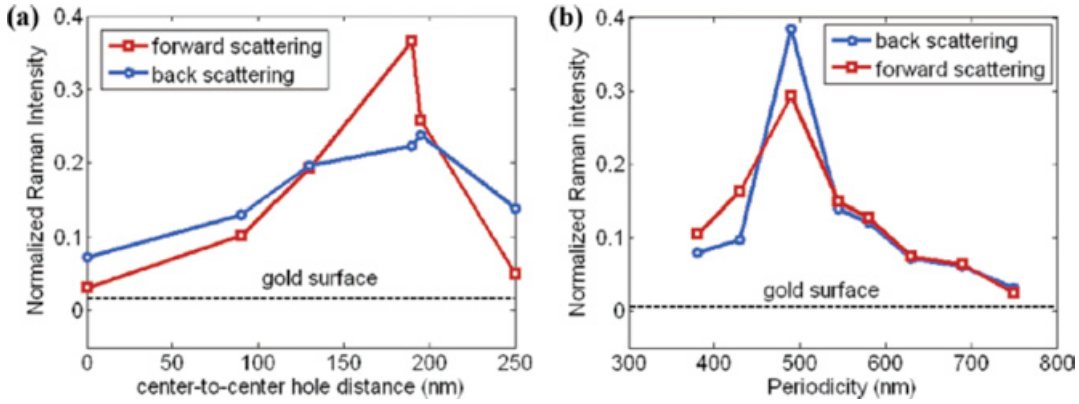

Figure 19 (online color at: www.lpr-journal.org) Raman scattering from arrays of double-holes. a) Maximum SERS observed in forward and back scattering geometries when the double-holes just overlapped to produce sharp apexes. b) Tuning the periodicity could further enhance the SERS. (Reprinted with permission from [200], © 2007 American Chemical Society)

uation of the EF from nanoholes in silver was carried out and a 10^2 enhancement due exclusively to the SP excitation through nanoholes was obtained [198]. SERS from a thin metal film covered with a random distribution of 50 nm nanoholes (coverage equals to 100 holes/μm^2) have been reported [199] and the obtained SERS signal was comparable to that obtained from individual nanoparticles.

The SERS results with circular holes show that the EF can be tuned by the array periodicity, but the magnitude of the enhancement is modest for those structures (between 10^2–10^4). The SERS efficiency can be further optimized by modifying the shape of the nanohole. As described in Sect. 3.3, the double-hole structure allows for strong local field enhancement when the holes are just touching to produce sharp apexes. The strong field enhancement in this double-hole structure was used to enhance SERS [200], as shown in Fig. 19. The extra enhancement from the localized SP at the apexes can be tuned by changing the double-hole center-to-center distance, which changes the shape of the apexes. The SERS enhancement factor from dyes adsorbed on the double-hole structure was an order of magnitude larger than for circular holes [200]. It should be kept in mind that the field enhancement only occurs over a much smaller area in the double-hole structure, so the enhancement is only "felt" by a small fraction of the molecules covering the surface. Therefore, when normalizing to the number of molecules in the field-enhanced regions, the SERS enhancement for double-holes is much greater.

3.7. Absorption spectroscopy

The ability of the subwavelength hole arrays to enhance absorption has been explored in infrared spectroscopy [10, 201–204]. A 300-fold increase in the infrared absorption relative to reflection-absorption spectroscopy has been reported for a self-assembled monolayer on copper, using transmission mode Fourier transform infrared spectroscopy. Besides the standard field enhancement effect common to any surface plasmon enhanced spectroscopic methods, another important contribution in the case of infrared absorption is the increase in path length enabled by SPPs that travel parallel to the metallic surface [204]. The analysis of the enhanced surface infrared spectrum of adsorbed species allow the determination of the orientation of molecular species with a higher precision due to the better signal-to-noise ratio than observed from reflection-absorption spectroscopy. The hole-enhanced infrared technique has been used to follow the catalytic conversion of methanol to formaldehyde and to study membrane proteins in phospholipid bilayers. In an interesting series of experiments, arrays were stacked to provide zero open area, and enhanced transmission was observed even in that situation. The resonances in this case were narrower than observed from individual arrays [205, 206]. This procedure can be used to obtain enhanced infrared absorption of thin films between the arrays. Based on these enhanced-absorption investigations, it is possible that hole-arrays will also find applications in photovoltaics.

3.8. Quantum effects

A few works have hinted at the possibility of enhanced quantum interactions using nanohole arrays. It was shown that entanglement could be preserved in the transmission of photons through nanohole arrays [207]. Since the enhanced transmission is enabled by the interaction with a sea of electrons in the metal, the quantum system interacts strongly with a large population of electrons, yet maintains its quantum coherence. Entanglement was preserved so long as care is taken to ensure that "which-path" information is not contained in the polarization state of the array. A second work has shown that quantum dots can have enhanced fluorescence by a factor of 300 when placed at the surface of the nanohole array [208]. Further work is required to harness the potential of enhanced quantum interactions allowed by nanoholes in metals, especially considering the metal loss

and the correspondingly low quality of resonances. Yet, as described above, nanohole arrays allow for resonantly focusing light down to the nanoscale, where reduced volumes and an increased local photon density of states show potential for enhanced quantum interactions [209].

3.9. Summary

Hole-arrays in metal films have brought new methods for polarization control, filtering, optical switching and sensing. They have allowed for enhanced interactions with materials, with applications in nonlinear optics, Raman spectroscopy and absorption spectroscopy. For these applications, the hole-array represents a compact structure for resonantly enhanced performance. Future refinements may bring even greater performance in these areas, for example, to detect and identify single molecules. In addition, the enhanced matter interaction allowed by hole-arrays is promising for the study of quantum effects, which have been relatively unexplored to date. For many of these applications, it is necessary to develop fabrication methodologies, especially for wide-scale deployment. In addition, the integration of hole-arrays into device platforms provides many challenges and opportunities. Fabrication and integration will be addressed in the next section.

4. Fabrication and integration

4.1. Fabrication approaches

The fabrication of hole-arrays for infrared and longer wavelengths does not require nanofabrication, and commercial meshes are readily available. Nevertheless, creative approaches can be used to obtain interesting features. As an example for arrays used in THz studies, a saw was used to cut rows of lines on either side of a silicon wafer. The rows were orthogonal to each other and when they intersected they produced square holes down to 45 μm [210].

For the use of hole-arrays in the optical and near-infrared, nanofabrication approaches are required. Early work on the fabrication of hole-arrays in metals (for the development of NSOM applications) used electron beam lithography [5, 6], and this method is still used in some cases, for example, in combination with sputter etching [186, 211]. Focused-ion beam (FIB) milling [212] has been used extensively to create hole-arrays [7]. FIB milling can be used to directly remove material from a metal film with high-resolution using gallium ions accelerated with voltages of around 30 keV and focused to ablate a surface on impact. In the past 10 years, FIB columns have been combined with scanning electron microscopes producing dual-beam systems, so that the milled structure can be inspected directly after milling. This allows for *in-situ* adaptation of the milling parameters to improve the nanostructure quality. FIB milling allows for spot sizes at the nanometer scale, and feature sizes of tens of nanometers are created routinely. FIB has also been used extensively on nickel films, which can be subsequently coated with noble metals to produce free-standing structures [41].

Photolithographic approaches have also been used to create hole arrays. It is possible to use the photoresist film to support membranes, and to produce holes of 5 micron diameter [213]. For smaller hole-sizes, it is possible to use interference lithography or phase-shifting photolithography, and subsequent deposition or etching of metal, to produce long range periodic structures [48, 90, 214, 215]. For sub-wavelength feature sizes, this approach commonly uses a UV laser ($\sim$ 365 nm) and produces features down to 150 nm. Even finer features can be obtained by creative interference lithographic approaches, such as undercut etching to produce fine annular apertures with gap-sizes of 60 nm [90]. Dual-period, elliptical, and half-elliptical structures have been produced with interference lithography over large areas [216].

Molding and printing techniques are also possible candidates for the creation of nanohole arrays over large areas – these techniques are potentially less-expensive and more rapid [217]. Soft nanoimprint lithography has been used to produce plasmonic sensors [218]. Replica techniques produce smooth surface nanohole arrays with higher-quality resonances [175]. Scanning probe methods are also possible, such as dip-pen nanolithography direct etching [219] and scanning probe nanolithography using mechanical force to create subwavelength hole arrays [220].

The most common bottom-up approach for the fabrication of nanohole arrays is the use of self-assembled polystyrene spheres as a template [221]. Organized domains of hexagonally packed spheres provide a template for subwavelength hole-arrays. Further processing includes plasma etching of the array of polystyrene spheres and metal deposition to produce holes. The metal deposition step can be either by physical deposition or by electrochemical deposition. The structure of the plasmonic substrate can be tuned by varying the diameter of the spheres, the etching, and deposition conditions. This approach allows the fabrication of arrays of either holes or particles. For instance, this fabrication method has been used to study the transition from localized SPR from isolated metallic nanoparticles to propagating SP waves characteristic of periodic hole arrays [222]. Many permutations are possible with polystyrene sphere lithography; for instance, nanowells, where a disk is below the hole, were fabricated using this procedure and studied in reflection and transmission modes [223].

4.2. Integration and devices

Arrays of holes in metal films, as sensors, are well-suited to device-level integration. The small foot print and normal collinear optical excitation mode were noted as motivating factors from the first sensing demonstration [163]. Since

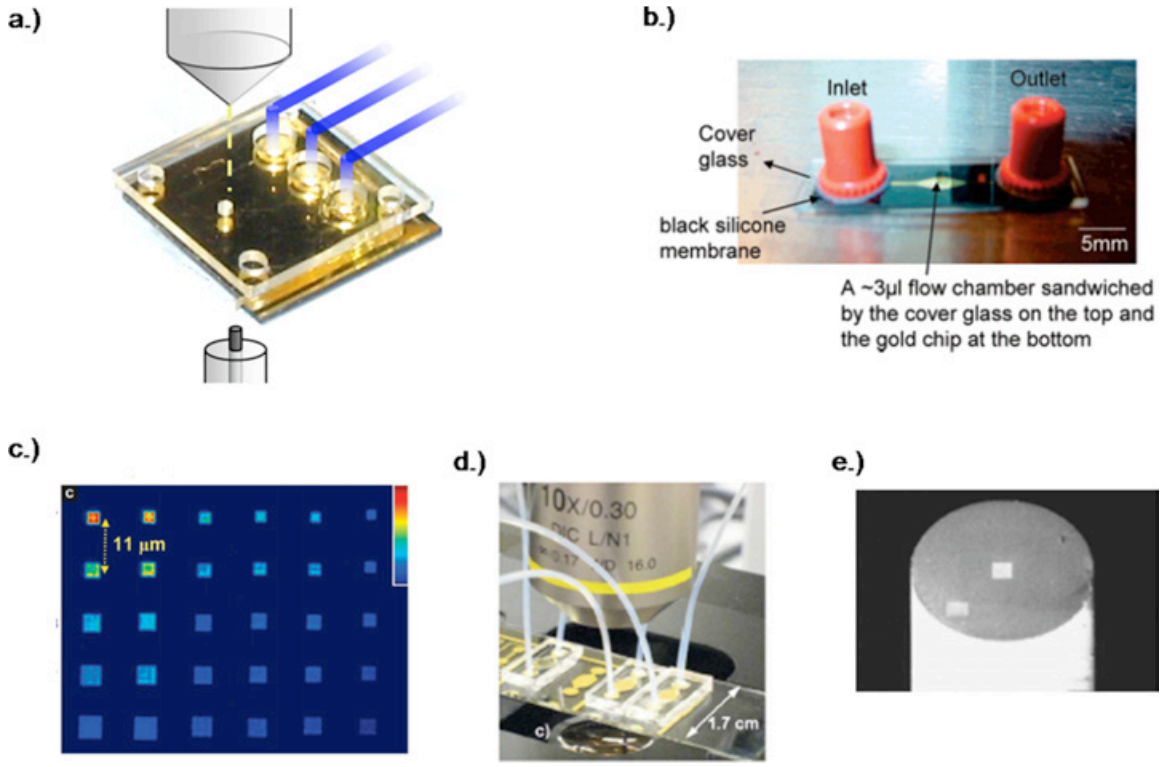

Figure 20 (online color at: www.lpr-journal.org) Examples of several microfluidic and optical integration strategies employed for nanohole array based sensors. a) An array of nanoholes arrays in a microfluidic chip (From [226], © 2007 American Chemical Society). b) A microfluidic platform with an array of 25 nanoholes arrays (From [211], © 2008 American Chemical Society). c) A 6×5 array of nanohole arrays used in real-time refractive index monitoring (From [175], © 2008 American Chemical Society). d) A set of microfluidic chips with integrated nanohole arrays using a single wavelength source and transmission intensity measurement (From [172], © 2008 Optical Society of America). e) An alternative, probe-style integration of nanoholes on the end of a fiber optic (From [228], © 2007 American Institute of Physics). (Reprints with permission)

that time, integration of nanohole arrays in a simple microfluidic channel has become relatively common. Recently, more intricate integration in terms of both fluidics and optics has been employed as the technology matures and some efforts shift from fundamentals toward applications. Integration efforts to date have largely been in concert with sensor developments and it is difficult to separate them entirely. A recent review discusses nanohole arrays as combined optofluidic (optical and fluidic) elements [224]. In this Section, an overview of the most notable integration advances to date is provided, as well as some areas for future efforts.

A common scenario involves, as a starting point, an array of nanoholes milled into a metal film on a flat macroscale substrate such as a glass slide. Employing a simple microfluidic channel over the array is the most basic form of integration and enables the local nanohole array environment to be protected, physically and chemically [165, 186]. A high aspect ratio rectangular cross-section microchannel also provides a means of exposing the sensor to a liquid environment without any of the flow or optical artifacts associated with a free liquid surface. Soft lithography is a common microfluidic channel fabrication strategy that is well suited to this application as it requires minimal infrastructure, cost and time [225]. In addition, the elastomeric nature of the chip (commonly polydimethylsiloxane, PDMS) facilitates reversible sealing to the glass or gold substrate that may be enforced through mechanical clamping, or may be irreversibly sealed to bare glass. Reversible sealing is convenient in many research applications involving nanopatterned substrates as the substrate may be removed, cleaned and reused multiple times while the chips are prone to contamination. The elastomeric nature of the chip also mitigates potential for damage to the arrays that can be incurred, for instance, in aligning the chip.

Fig. 20 shows examples of several microfluidic and optical integration strategies employed for nanohole arrays in metal films. An integrated chip with a 6×2 array of nanohole arrays that facilitated spatial detection of a concentration gradient and sequential detection of biotin and streptavidin [226] is shown in Fig. 20a. More recently, an array of 25 individual nanohole arrays was integrated in a microfluidic platform as shown in Fig. 20b, and 25 separate binding curves were obtained for the same adsorption system [211]. Similarly, Yang and coworkers [175] employed an integrated 6×5 array of nanoholes arrays as shown in

Fig. 20c. In that work, multiplexed nanohole arrays, of size down to 3×3 holes, were used in the real-time refractive index monitoring and the detection of a SAM and anti-G surface-binding [175]. Refractive index matching in that work allowed for 20% improved sensing performance and the supersmooth surface allowed for reduced scattering losses and sharper peaks. Furthermore, the holes were created using a replication technique which shows promise for mass-production. Both these studies, as well as Lesuffleur et al [167], shown in Fig. 20d, employed a single wavelength source, and thus measured a change in transmission intensity at each array as opposed to spectral data. As discussed earlier in this paper, direct intensity measurements can take advantage of parallelized detectors such as CCDs and thus can achieve a higher degree of multiplexing and throughput than spectral measurements obtained serially [172, 175, 211].

Other strategies for integration of nanohole arrays have been developed. One interesting approach that deviates from the lab-on-chip concept is to integrate nanoholes on the end of a fiber [227, 228], as shown in Fig. 20e. Such a device could potentially be used in vivo for a range of diagnostic purposes, however, environmental control (rinsing etc.) that is important for surface adsorption tests would be a challenge in the fiber-optic approach.

The maximum achievable density of array-based sensors in a planar device depends on several factors: the ability to independently functionalize and address each sensor with analyte and sensing optics and the minimum size of array. Regarding the minimum size, recent demonstrations realized sensing with nanohole arrays as small as 1 μm^2. Edge effects become more important at small array sizes. It is possible, for instance, to isolate separate arrays, as well as enhance EOT by capturing SPs that are travelling away at the edges of the array. This isolation has been achieved using grooves or dimples called plasmonic Bragg reflectors [229, 230].

To date, nanohole integration strategies have involved dead-ended holes, or pits, in a solid substrate. In those cases, integration efforts developed previously for other localized surface sensors, such as microarrays, are readily applicable. A flow-through nanohole array scheme, as discussed previously, exhibits several advantages in terms of analyte transport and solution sieving [12]. Integration with flow-through nanohole arrays, however, will involve some additional challenges and opportunities. For instance, to achieve through nanoholes, very thin, and stiff materials, such as silicon nitride are required. Such a flow-through film requires integration with service fluidics on both top and bottom. With these challenges met, extension to multiplexing, in plane, should be straightforward.

Looking ahead, it is possible to foresee many potential developments in this area. The normal incidence interrogation mode, inherent to nanohole arrays, rules out three-dimensional integration since direct optical access is required on both sides. However, the degree of planar integration may be greatly increased beyond current demonstrations. It is also likely that new alternative approaches, such as the fiber integration and the flow-through nanohole array, will appear and present new integration challenges and opportunities. Many developments in this area are expected as nanohole array-based sensing technology matures.

4.3. Summary

Among the many fabrication approaches for hole-arrays, both top-down and bottom-up, several show promise for mass fabrication. In addition, there are many possibilities for the integration of hole-arrays into device platforms. In some cases, the hole-arrays can provide additional functionality beyond the resonant optical transmission; for example, by acting as fluidic channels for a solution of analyte. It is clear that there are many possibilities for multidisciplinary collaboration to advance the hole-array based devices and applications.

5. Outlook

The field study of hole-arrays in metal films has undergone intense advancement in the last decade, since the report of Ebbesen and co-workers of extraordinary optical transmission. The physics of this transmission phenomenon has been studied in depth, and a good body of literature has amassed on the influence of various metals, wavelengths and structural parameters on the transmission resonance. Nevertheless, there are still vigorous debates in the literature about the exact causes of this phenomenon.

Further growth is expected in this research area for years to come. This growth will be led by the many potential applications to photonics. Already, the research on hole-arrays is a multi-disciplinary topic, involving researchers in physics, chemistry, engineering, biology and medical sciences. The intermixing between these fields will introduce different approaches and more applications for hole-arrays.

Two other factors support further growth in this field. First, there has been considerable advancement in the technology to create large-area hole-arrays at the nanoscale using inexpensive and efficient technologies. The advancement of nanofabrication will provide greater access to nanohole arrays to researchers in various fields. Second, the computational power to solve complex problems of electromagnetism with realistic material properties are now inexpensive enough to be open to almost every researcher in the field. Many in-house and commercial software packages have been employed to study the nuisances of various hole-arrays, and this has lead to several new designs. As the trends of improved nanofabrication and accessible computational electromagnetics continue, the research on hole arrays in metal films is expected to grow as well.

Acknowledgements The authors acknowledge the support of NSERC, CIPI, CFI, BCKDF, Micralyne, BC Cancer Agency Trev and Joyce Deeley Research Centre, and CAMTEC.

Reuven Gordon received his B. A. Sc. and M. A. Sc. from the University of Toronto (Canada). He received his Ph. D. in Physics from the University of Cambridge (UK) in 2002, and he was co-inventor of transverse mode-locking within the Hitachi Cambridge Laboratory. In 2002, he joined the University of Victoria (Canada), where he currently holds an associate professor position in the Department of Electrical and Computer Engineering. His research group is mainly interested in the optical properties and applications of nanostructured metals.

Alexandre G. Brolo received his M. Sc. from the University of Sao Paulo (Brazil). He then moved to Canada and obtained his Ph. D. from the University of Waterloo (Canada), while working on the application of surface-enhanced Raman scattering to study electrochemical processes. He is now an associate professor of Chemistry at the University of Victoria (Canada). His current interests are on the application of "in situ" spectroscopic methods to study electrochemical systems, and on the development of substrates for enhanced spectroscopy, chemical sensing and nano-photonics.

David Sinton studied mechanical engineering at the University of Toronto (Canada) and McGill University (Canada). He achieved his Ph. D. at the University of Toronto in the area of microfluidics. He is currently an associate professor in the Dept. of Mechanical Engineering at the University of Victoria (Canada). The Sinton Research Group focuses on the study of transport phenomena in micro- and nanostructures and the integration of optics and fluidics.

Karen L. Kavanagh earned her Ph. D. in Materials Science and Engineering from Cornell University in 1987 working on interdiffusion and defects at III-V semiconductor interfaces. As a post-doctoral fellow at IBM T. J. Watson Laboratory and MIT she investigated strain associated with dopant impurities in silicon using x-ray scattering. From 1988 to 1999 she was a Professor of Electrical and Computer Engineering at the University of California, San Diego, where she established a lab working on strain relaxation in lattice-mismatched semiconductor interfaces and ballistic electron transport at metal-semiconductor interfaces. Since 2000 she has been a Professor of Physics at Simon Fraser University where she has concentrated on nanoscience and technology including investigations of integrated circuit reliability, transparent conducting oxides, atomic ordering,epitaxial contacts by electrodeposition, semiconductor nanowires, and optical properties of nanohole arrays.

References

[1] Lord Rayleigh, Philos. Mag. **14**, 60 (1907).
[2] H. A. Bethe, Phys. Rev. **66**, 163 (1944).
[3] C. J. Bouwkamp, Philips Res. Rep. **5**, 401 (1950).
[4] K. F. Renk and L. Genzel, Appl. Opt. **1**, 643 (1962).
[5] A. Lewis, M. Isaacson, A. Harootunian, and A. Murray, Ultramicroscopy **13**, 227 (1984).
[6] E. Betzig, A. Lewis, A. Harootunian, M. Isaacson, and E. Kratschmer, J. Biophys. **49**, 269 (1986).
[7] T. W. Ebbesen, H. J. Lezec, H. F. Ghaemi, T. Thio, and P. A. Wolff, Nature **391**, 667 (1998).
[8] F. J. G. de Abajo, Rev. Mod. Phys. **79**, 1267 (2007).
[9] C. Genet and T. W. Ebbesen, Nature **445**, 39 (2007).
[10] J. V. Coe, J. M. Heer, S. Teeters-Kennedy, H. Tian, and K. R. Rodriguez, Ann. Rev. Phys. Chem. **59**, 179 (2008).
[11] M. E. Stewart, C. R. Anderton, L. B. Thompson, J. Maria, S. K. Gray, J. A. Rogers, and R. G. Nuzzo, Chem. Rev. **108**, 494 (2008).
[12] R. Gordon, D. Sinton, K. L. Kavanagh, and A. G. Brolo, Acc. Chem. Res. **41**, 1049 (2008).
[13] J. D. Jackson, Classical Electrodynamics (Wiley, New York, 1998).
[14] R. Gordon and A. G. Brolo, Opt. Express **13**, 1933 (2005).
[15] A. Degiron, H. J. Lezec, N. Yamamoto, and T. W. Ebbesen, Opt. Commun. **239**, 61 (2004).
[16] P. B. Catrysse, H. Shin, and S. H. Fan, J. Vacuum Sci. Technol. B **23**, 2675 (2005).
[17] H. Shin, P. B. Catrysse, and S. Fan, Phys. Rev. B **72**, 085436 (2005).
[18] R. Ulrich, Infrared Phys. **7**, 37 (1967).
[19] G. M. Ressler and K. D. Moller, Appl. Opt. **6**, 893 (1967).
[20] A. Mitsuishi, Y. Otsuka, S. Fujita, and H. Yoshinaga, Jpn. J. Appl. Phys. **2**, 574 (1963).
[21] C. C. Chen, IEEE Trans. Microw. Theory Tech. **19**, 475 (1971).
[22] C. C. Chen, IEEE Trans. Microw. Theory Tech. **18**, 627 (1970).
[23] S. W. Lee, G. Zarrillo, and C. L. Law, IEEE Trans. Antennas Propag. **30**, 904 (1982).
[24] R. E. Collin and W. H. Eggimann, IRE Trans. Microw. Theory Tech. **9**, 110 (1961).
[25] J. B. Masson, A. Podzorov, and G. Gallot, Opt. Express **16**, 4719 (2008).
[26] F. J. G. de Abajo, R. Gomez-Medina, and J. J. Saenz, Phys. Rev. E **72**,16608 (2005).

[27] R. Gordon, Phys. Rev. A **76**, 053806 (2007).
[28] C. Genet, M. P. van Exter, and J. P. Woerdman, Opt. Commun. **225**, 331 (2003).
[29] M. Sarrazin, J. P. Vigneron, and J. M. Vigoureux, Phys. Rev. B **67**, 085415 (2003).
[30] R. Muller, C. Ropers, and C. Lienau, Opt. Express **12**, 5067 (2004).
[31] H. F. Ghaemi, T. Thio, D. E. Grupp, T. W. Ebbesen, and H. J. Lezec, Phys. Rev. B **58**, 6779 (1998).
[32] M. M. J. Treacy, Phys. Rev. B **66**, 195105 (2002).
[33] Q. Cao and P. Lalanne, Phys. Rev. Lett. **88**, 057403 (2002).
[34] E. Popov, S. Enoch, G. Tayeb, M. Neviere, B. Gralak, and N. Bonod, Appl. Opt. **43**, 999 (2004).
[35] H. J. Lezec and T. Thio, Opt. Express **12**, 3629 (2004).
[36] G. Gay, O. Alloschery, B. V. De Lesegno, C. O'Dwyer, J. Weiner, and H. J. Lezec, Nature Phys. **2**, 262 (2006).
[37] P. Lalanne and J. P. Hugonin, Nature Phys. **2**, 551 (2006).
[38] S. Selcuk, K. Woo, D. B. Tanner, A. F. Hebard, A. G. Borisov, and S. V. Shabanov, Phys. Rev. Lett. **97**, 067403 (2006).
[39] H. T. Liu and P. Lalanne, Nature **452**, 728 (2008).
[40] W. L. Barnes, W. A. Murray, J. Dintinger, E. Devaux, and T. W. Ebbesen, Phys. Rev. Lett. **92**, 107401 (2004).
[41] D. E. Grupp, H. J. Lezec, T. W. Ebbesen, K. M. Pellerin, and T. Thio, Appl. Phys. Lett. **77**, 1569 (2000).
[42] F. Przybilla, A. Degiron, J. Y. Laluet, C. Genet, and T. W. Ebbesen, J. Opt. A, Pure Appl. Opt. **8**, 458 (2006).
[43] S. G. Rodrigo, F. J. García-Vidal, and L. Martín-Moreno, Phys. Rev. B **77**, 075401 (2008).
[44] M. Sarrazin and J. P. Vigneron, Phys. Rev. E **68**, 016603 (2003).
[45] T. Thio, H. F. Ghaemi, H. J. Lezec, P. A. Wolff, and T. W. Ebbesen, J. Opt. Soc. Am. B, Opt. Phys. **16**, 1743 (1999).
[46] S. C. Hohng, Y. C. Yoon, D. S. Kim, V. Malyarchuk, R. Muller, C. Lienau, J. W. Park, K. H. Yoo, J. Kim, H. Y. Ryu, and Q. H. Park, Appl. Phys. Lett. **81**, 3239 (2002).
[47] D. S. Kim, S. C. Hohng, V. Malyarchuk, Y. C. Yoon, Y. H. Ahn, K. J. Yee, J. W. Park, J. Kim, Q. H. Park, and C. Lienau, Phys. Rev. Lett. **91**, 143901 (2003).
[48] E. S. Kwak, J. Henzie, S. H. Chang, S. K. Gray, G. C. Schatz, and T. W. Odom, Nano Lett. **5**, 1963 (2005).
[49] H. T. Gao, H. F. Shi, C. T. Wang, C. L. Du, X. G. Luo, Q. L. Deng, Y. G. Lv, X. D. Lin, and H. M. Yao, Opt. Express **13**, 10795 (2005).
[50] Y. Poujet, M. Roussey, J. Salvi, F. I. Baida, D. Van Labeke, A. Perentes, C. Santschi, and P. Hoffmann, Photon. Nanostructures, Fundam. Appl. **4**, 47 (2006).
[51] J. Y. Chu, T. J. Wang, J. T. Yeh, M. W. Lin, Y. C. Chang, and J. K. Wang, Appl. Phys. A, Mater. Sci. Process. **89**, 387 (2007).
[52] M. H. Chowdhury, J. M. Catchmark, and J. R. Lakowicza, Appl. Phys. Lett. **91**, 103118 (2007).
[53] H. W. Gao, J. Henzie, and T. W. Odom, Nano Lett. **6**, 2104 (2006).
[54] L. Salomon, F. D. Grillot, A. V. Zayats, and F. de Fornel, Phys. Rev. Lett. **86**, 1110 (2001).
[55] H. Cao and A. Nahata, Opt. Express **12**, 1004 (2004).
[56] W. Zhang, Eur. Phys. J., Appl. Phys. **43**, 1 (2008).
[57] D. X. Qu and D. Grischkowsky, Phys. Rev. Lett. **93**, 196804 (2004).
[58] D. X. Qu, D. Grischkowsky, and W. L. Zhang, Opt. Lett. **29**, 896 (2004).
[59] A. K. Azad, Y. G. Zhao, W. L. Zhang, and M. X. He, Opt. Lett. **31**, 2637 (2006).
[60] D. Korobkin, Y. A. Urzhumov, B. Neuner, C. Zorman, Z. Zhang, I. D. Mayergoyz, and G. Shvets, Appl. Phys. A, Mater. Sci. Process. **88**, 605 (2007).
[61] J. G. Rivas, C. Schotsch, P. H. Bolivar, and H. Kurz, Phys. Rev. B **68**, 201306 (2003).
[62] J. G. Rivas, C. Janke, P. H. Bolivar, and H. Kurz, Opt. Express **13**, 847 (2005).
[63] M. Beruete, M. Sorolla, I. Campillo, J. S. Dolado, L. Martín-Moreno, J. Bravo-Abad, and F. J. García-Vidal, Opt. Lett. **29**, 2500 (2004).
[64] B. Hou, Z. H. Hang, W. J. Wen, C. T. Chan, and P. Sheng, Appl. Phys. Lett. **89**, 131917 (2006).
[65] X. Shou, A. Agrawal, and A. Nahata, Opt. Express **13**, 9834 (2005).
[66] A. Degiron, H. J. Lezec, W. L. Barnes, and T. W. Ebbesen, Appl. Phys. Lett. **81**, 4327 (2002).
[67] F. J. García-Vidal, E. Moreno, J. A. Porto, and L. Martín-Moreno, Phys. Rev. Lett. **95**, 103901 (2005).
[68] J. B. Pendry, L. Martín-Moreno, and F. J. García-Vídal, Sci. **305**, 847 (2004).
[69] E. Popov, M. Neviere, S. Enoch, and R. Reinisch, Phys. Rev. B **62**, 16100 (2000).
[70] S. Enoch, E. Popov, M. Neviere, and R. Reinisch, J. Opt. A, Pure Appl. Opt. **4**, S83 (2002).
[71] L. Martín-Moreno, F. J. García-Vidal, H. J. Lezec, K. M. Pellerin, T. Thio, J. B. Pendry, and T. W. Ebbesen, Phys. Rev. Lett. **86**, 1114 (2001).
[72] R. Gordon, L. K. S. Kumar, and A. G. Brolo, IEEE Trans. Nanotechnol. **5**, 291 (2006).
[73] F. J. García-Vidal, L. Martín-Moreno, E. Moreno, L. K. S. Kumar, and R. Gordon, Phys. Rev. B **74**, 153411 (2006).
[74] M. C. Hughes and R. Gordon, Appl. Phys. B, Lasers Opt. **87**, 239 (2007).
[75] Z. C. Ruan and M. Qiu, Phys. Rev. Lett. **96**, 233901 (2006).
[76] A. Mary, S. G. Rodrigo, L. Martín-Moreno, and F. J. García-Vidal, Phys. Rev. B **76**, 195414 (2007).
[77] S. M. Orbons and A. Roberts, Opt. Express **14**, 12623 (2006).
[78] S. M. Williams, A. D. Stafford, T. M. Rogers, S. R. Bishop, and J. V. Coe, Appl. Phys. Lett. **85**, 1472 (2004).
[79] F. J. G. de Abajo and J. J. Saenz, Phys. Rev. Lett. **95**, 233901 (2005).
[80] A. P. Hibbins, M. J. Lockyear, I. R. Hooper, and J. R. Sambles, Phys. Rev. Lett. **96**, 073904 (2006).
[81] A. V. Kats, M. L. Nesterov, and A. Y. Nikitin, Phys. Rev. B **76**, 045413 (2007).
[82] A. Roberts and R. C. McPhedran, IEEE Trans. Antennas Propag. **36**, 607 (1988).
[83] F. I. Baida, A. Belkhir, D. Van Labeke, and O. Lamrous, Phys. Rev. B **74**, 205419 (2006).
[84] M. I. Haftel, C. Schlockermann, and G. Blumberg, Phys. Rev. B **74**, 235405 (2006).
[85] S. M. Orbons, A. Roberts, D. N. Jamieson, M. I. Haftel, C. Schlockermann, D. Freeman, and B. Luther-Davies, Appl. Phys. Lett. **90**, 251107 (2007).

[86] F. I. Baida and D. Van Labeke, Opt. Commun. **209**, 17 (2002).
[87] F. I. Baida and D. Van Labeke, Phys. Rev. B **67**, 155314 (2003).
[88] J. Salvi, M. Roussey, F. I. Baida, M. P. Bernal, A. Mussot, T. Sylvestre, H. Maillotte, D. Van Labeke, A. Perentes, I. Utke, C. Sandu, P. Hoffmann, and B. Dwir, Opt. Lett. **30**, 1611 (2005).
[89] W. J. Fan, S. Zhang, B. Minhas, K. J. Malloy, and S. R. J. Brueck, Phys. Rev. Lett. **94**, 033902 (2005).
[90] W. J. Fan, S. Zhang, K. J. Malloy, and S. R. J. Brueck, Opt. Express **13**, 4406 (2005).
[91] A. Moreau, G. Granet, F. I. Baida, and D. Van Labeke, Opt. Express **11**, 1131 (2003).
[92] R. Gordon, A. G. Brolo, A. McKinnon, A. Rajora, B. Leathem, and K. L. Kavanagh, Phys. Rev. Lett. **92**, 037401 (2004).
[93] K. J. K. Koerkamp, S. Enoch, F. B. Segerink, N. F. van Hulst, and L. Kuipers, Phys. Rev. Lett. **92**, 183901 (2004).
[94] K. L. van der Molen, F. B. Segerink, N. F. van Hulst, and L. Kuipers, Appl. Phys. Lett. **85**, 4316 (2004).
[95] K. L. van der Molen, K. J. Klein Koerkamp, S. Enoch, F. B. Segerink, N. F. van Hulst, and L. Kuipers, Phys. Rev. B **72**, 045421 (2005).
[96] M. Sarrazin and J. P. Vigneron, Opt. Commun. **240**, 89 (2004).
[97] X. F. Ren, P. Zhang, G. P. Guo, Y. F. Huang, Z. W. Wang, and G. C. Guo, Appl. Phys. B, Lasers Opt. **91**, 601 (2008).
[98] Y. M. Strelniker, Phys. Rev. B **76**, 085409 (2007).
[99] J. B. Masson and G. Gallot, Phys. Rev. B **73**, 121401 (2006).
[100] H. Cao and A. Nahata, Opt. Express **12**, 3664 (2004).
[101] R. Gordon, M. Hughes, B. Leathem, K. L. Kavanagh, and A. G. Brolo, Nano Lett. **5**, 1243 (2005).
[102] A. Degiron and T. W. Ebbesen, J. Opt. A, Pure Appl. Opt. **7**, S90 (2005).
[103] R. C. Compton, R. C. McPhedran, G. H. Derrick, and L. C. Botten, Infrared Phys. **23**, 239 (1983).
[104] C. Y. Chen, M. W. Tsai, T. H. Chuang, Y. T. Chang, and S. C. Lee, Appl. Phys. Lett. **91**, 063108 (2007).
[105] R. M. Roth, N. C. Panoiu, M. M. Adams, J. I. Dadap, and R. M. Osgood, Opt. Lett. **32**, 3414 (2007).
[106] Y. H. Ye, Z. B. Wang, D. S. Yan, and J. Y. Zhang, Opt. Lett. **32**, 3140 (2007).
[107] M. Airola, Y. Liu, and S. Blair, J. Opt. A, Pure Appl. Opt. **7**, S118 (2005).
[108] T. Xu, X. Jiao, G. P. Zhang, and S. Blair, Opt. Express **15**, 13894 (2007).
[109] J. H. Kim and P. J. Moyer, Appl. Phys. Lett. **89**, 121106 (2006).
[110] E. Jin and X. Xu, J. Quant. Spectrosc. Radiat. Transf. **93**, 163 (2005).
[111] J. W. Lee, M. A. Seo, D. J. Park, D. S. Kim, S. C. Jeoung, C. Lienau, Q. H. Park, and P. C. M. Planken, Opt. Express **14**, 1253 (2006).
[112] M. Sun, R. J. Liu, Z. Y. Li, B. Y. Cheng, D. Z. Zhang, H. F. Yang, and A. Z. Jin, Phys. Lett. A **365**, 510 (2007).
[113] L. K. S. Kumar and R. Gordon, IEEE J. Sel. Top. Quantum Electron. **12**, 1228 (2006).
[114] L. K. S. Kumar, A. Lesuffleur, M. C. Hughes, and R. Gordon, Appl. Phys. B, Lasers Opt. **84**, 25 (2006).
[115] A. Battula, Y. L. Lu, R. J. Knize, K. Reinhardt, and S. C. Chen, Opt. Express **15**, 14629 (2007).
[116] F. Miyamaru and M. Hangyo, Phys. Rev. B **72**, 035429 (2005).
[117] F. Miyamaru and M. Hangyo, Appl. Phys. Lett. **89**, 211105 (2006).
[118] X. F. Ren, G. P. Guo, Y. F. Huang, Z. W. Wang, and G. C. Guo, Appl. Phys. Lett. **90**, 161112 (2007).
[119] E. Altewischer, M. P. van Exter, and J. P. Woerdman, J. Opt. Soc. Am. B, Opt. Phys. **20**, 1927 (2003).
[120] E. Altewischer, M. P. van Exter, and J. P. Woerdman, J. Opt. Soc. Am. B, Opt. Phys. **22**, 1731 (2005).
[121] A. V. Kats, M. L. Nesterov, and A. Y. Nikitin, Phys. Rev. B **72**, 193405 (2005).
[122] X. F. Ren, G. P. Guo, Y. F. Huang, Z. W. Wang, and G. C. Guo, Opt. Lett. **31**, 2792 (2006).
[123] J. Bravo-Abad, F. J. García-Vidal, and L. Martín-Moreno, Phys. Rev. Lett. **93**, 227401 (2004).
[124] Y. Alaverdyan, B. Sepulveda, L. Eurenius, E. Olsson, and M. Kall, Nature Phys. **3**, 884 (2007).
[125] J. Bravo-Abad, A. Degiron, F. Przybilla, C. Genet, F. J. García-Vidal, L. Martín-Moreno, and T. W. Ebbesen, Nature Phys. **2**, 120 (2006).
[126] F. Miyamaru and M. Hangyo, Appl. Phys. Lett. **84**, 2742 (2004).
[127] F. Przybilla, C. Genet, and T. W. Ebbesen, Appl. Phys. Lett. **89**, 121115 (2006).
[128] M. Sun, J. Tian, S. Z. Han, Z. Y. Li, B. Y. Cheng, D. Z. Zhang, A. Z. Jin, and H. F. Yang, J. Appl. Phys. **100**, 024320 (2006).
[129] A. Agrawal, T. Matsui, Z. V. Vardeny, and A. Nahata, J. Opt. Soc. Am. B, Opt. Phys. **24**, 2545 (2007).
[130] T. Matsui, A. Agrawal, A. Nahata, and Z. V. Vardeny, Nature **446**, 517 (2007).
[131] J. Bravo-Abad, A. I. Fernandez-Dominguez, F. J. García-Vidal, and L. Martín-Moreno, Phys. Rev. Lett. **99**, 203905 (2007).
[132] F. M. Huang, N. Zheludev, Y. F. Chen, and F. J. G. de Abajo, Appl. Phys. Lett. **90**, 091119 (2007).
[133] Y. J. Bao, B. Zhang, Z. Wu, J. W. Si, M. Wang, R. W. Peng, X. Lu, J. Shao, Z. F. Li, X. P. Hao, and N. B. Ming, Appl. Phys. Lett. **90**, 251914 (2007).
[134] T. Onishi, T. Tanigawa, T. Ueda, and D. Ueda, IEEE J. Quantum Electron. **43**, 1123 (2007).
[135] P. Marthandam and R. Gordon, J. Opt. A, Pure Appl. Opt. **9**, 1140 (2007).
[136] P. J. Bliek, L. C. Botten, R. Deleuil, R. C. McPhedran, and D. Maystre, IEEE Trans. Microw. Theory Tech. **28**, 1119 (1980).
[137] R. C. McPhedran and D. Maystre, Appl. Phys. **14**, 1 (1977).
[138] M. U. Pralle, N. Moelders, M. P. McNeal, I. Puscasu, A. C. Greenwald, J. T. Daly, E. A. Johnson, T. George, D. S. Choi, I. El-Kady, and R. Biswas, Appl. Phys. Lett. **81**, 4685 (2002).
[139] R. Biswas, C. G. Ding, I. Puscasu, M. Pralle, M. McNeal, J. Daly, A. Greenwald, and E. Johnson, Phys. Rev. B **74**, 045107 (2006).
[140] M. W. Tsai, T. H. Chuang, C. Y. Meng, Y. T. Chang, and S. C. Lee, Appl. Phys. Lett. **89**, 173116 (2006).
[141] J. R. DiMaio and J. Ballato, Opt. Express **14**, 2380 (2006).

[142] C. L. Pan, C. F. Hsieh, R. P. Pan, M. Tanaka, F. Miyamaru, M. Tani, and M. Hangyo, Opt. Express **13**, 3921 (2005).
[143] Y. M. Strelniker, D. Stroud, and A. O. Voznesenskaya, Eur. Phys. J. B **52**, 1 (2006).
[144] Y. M. Strelniker and D. J. Bergman, Phys. Rev. B **59**, 12763 (1999).
[145] Y. M. Strelniker and D. J. Bergman, Phys. Rev. B **77**, 205113 (2008).
[146] C. Janke, J. G. Rivas, P. H. Bolivar, and H. Kurz, Opt. Lett. **30**, 2357 (2005).
[147] E. Hendry, M. J. Lockyear, J. G. Rivas, L. Kuipers, and M. Bonn, Phys. Rev. B **75**, 235305 (2007).
[148] W. Dickson, G. A. Wurtz, P. R. Evans, R. J. Pollard, and A. V. Zayats, Nano Lett. **8**, 281 (2008).
[149] J. Dintinger, S. Klein, and T. W. Ebbesen, Adv. Mater. **18**, 1267 (2006).
[150] A. Lesuffleur, L. K. S. Kumar, and R. Gordon, Appl. Phys. Lett. **88**, 261104 (2006).
[151] A. Lesuffleur, L. K. S. Kumar, and R. Gordon, Phys. Rev. B **75**, 045423 (2007).
[152] F. Eftekhari and R. Gordon, IEEE Sel. Top. Quantum Electron. **14**, 1552 (2008).
[153] J. A. H. van Nieuwstadt, M. Sandtke, R. H. Harmsen, F. B. Segerink, J. C. Prangsma, S. Enoch, and L. Kuipers, Phys. Rev. Lett. **97**, 146102 (2006).
[154] W. Fan, S. Zhang, N. C. Panoiu, A. Abdenour, S. Krishna, R. M. Osgood, K. J. Malloy, and S. R. J. Brueck, Nano Lett. **6**, 1027 (2006).
[155] A. Krishnan, T. Thio, T. J. Kima, H. J. Lezec, T. W. Ebbesen, P. A. Wolff, J. Pendry, L. Martín-Moreno, and F. J. García-Vidal, Opt. Commun. **200**, 1 (2001).
[156] J. Homola, Chem. Rev. **108**, 462 (2008).
[157] E. Kretschmann and H. Raether, Z. Nat.forsch. A, Astrophys. Phys. Phys. Chem. **23**, 2135 (1968).
[158] L. S. Jung, C. T. Campbell, T. M. Chinowsky, M. N. Mar, and S. S. Yee, Langmuir **14**, 5636 (1998).
[159] H. J. Lee, A. W. Wark, and R. M. Corn, Langmuir **22**, 5241 (2006).
[160] C. T. Campbell and G. Kim, Biomaterials **28**, 2380 (2007).
[161] A. D. Sheehan, J. Quinn, S. Daly, P. Dillon, and R. O'Kennedy, Anal. Lett. **36**, 511 (2003).
[162] N. Ramachandran, D. N. Larson, P. R. H. Stark, E. Hainsworth, and J. LaBaer, Febs J. **272**, 5412 (2005).
[163] A. G. Brolo, R. Gordon, B. Leathem, and K. L. Kavanagh, Langmuir **20**, 4813 (2004).
[164] J. M. Yao, M. E. Stewart, J. Maria, T. W. Lee, S. K. Gray, J. A. Rogers, and R. G. Nuzzo, Angew. Chem., Int. Ed. **47**, 5013 (2008).
[165] K. A. Tetz, L. Pang, and Y. Fainman, Opt. Lett. **31**, 1528 (2006).
[166] P. R. H. Stark, A. E. Halleck, and D. N. Larson, Methods **37**, 37 (2005).
[167] A. Lesuffleur, H. Im, N. C. Lindquist, and S. H. Oh, Appl. Phys. Lett. **90**, 243110 (2007).
[168] K. A. Tetz, R. Rokitski, M. Nezhad, and Y. Fainman, Appl. Phys. Lett. **86**, 111110 (2005).
[169] E. Altewischer, C. Genet, M. P. van Exter, J. P. Woerdman, P. F. A. Alkemade, A. van Zuuk, and E. van der Drift, Opt. Lett. **30**, 90 (2005).
[170] J. Homola, Surface Plasmon Resonance Based Sensors (Springer, Berlin, 2006).
[171] J. C. Sharpe, J. S. Mitchell, L. Lin, H. Sedoglavich, and R. J. Blaikie, Anal. Chem. **80**, 2244 (2008).
[172] A. Lesuffleur, H. Im, N. C. Lindquist, K. S. Lim, and S. H. Oh, Opt. Express **16**, 219 (2008).
[173] F. Eftekhari, R. Gordon, J. Ferreira, A. G. Brolo, and D. Sinton, Appl. Phys. Lett. **92**, 253103 (2008).
[174] J. Ferreira, M. J. L. Santos, M. M. Rahman, A. G. Brolo, R. Gordon, D. Sinton, and E. M. Girotto, J. Am. Chem. Soc. **131**, 436 (2009).
[175] J. C. Yang, J. Ji, J. M. Hogle, and D. N. Larson, Nano Lett. **8**, 2718 (2008).
[176] A. Dahlin, M. Zach, T. Rindzevicius, M. Kall, D. S. Sutherland, and F. Hook, J. Am. Chem. Soc. **127**, 5043 (2005).
[177] D. Gao, W. Chen, A. Mulchandani, and J. S. Schultz, Appl. Phys. Lett. **90**, 073901 (2007).
[178] F. Eftekhari, C. Escobedo, J. Ferreira, X. Duan, E. Girotto, A. G. Brolo, R. Gordon, and D. Sinton, Anal. Chem., ASAP DOI:10.1021/ac900221y (2009).
[179] M. Tanaka, F. Miyamaru, M. Hangyo, T. Tanaka, M. Akazawa, and E. Sano, Opt. Lett. **30**, 1210 (2005).
[180] K. R. Rodriguez, H. Tian, J. M. Heer, and J. V. Coe, J. Phys. Chem. C **111**, 12106 (2007).
[181] H. Yang and X. S. Xie, J. Chem. Phys. **117**, 10965 (2002).
[182] G. Ritchie and E. Burstein, Phys. Rev. B **24**, 4843 (1981).
[183] J. R. Lakowicz, K. Ray, M. Chowdhury, H. Szmacinski, Y. Fu, J. Zhang, and K. Nowaczyk, Analyst **133**, 1308 (2008).
[184] Y. D. Liu and S. Blair, Opt. Lett. **28**, 507 (2003).
[185] A. G. Brolo, S. C. Kwok, M. G. Moffitt, R. Gordon, J. Riordon, and K. L. Kavanagh, J. Am. Chem. Soc. **127**, 14936 (2005).
[186] Y. Liu, J. Bishop, L. Williams, S. Blair, and J. Herron, Nanotechnology **15**, 1368 (2004).
[187] Y. D. Liu, F. Mahdavi, and S. Blair, IEEE J. Sel. Top. Quantum Electron. **11**, 778 (2005).
[188] F. Mahdavi, Y. Liu, and S. Blair, Plasmonics **2**, 129 (2007).
[189] A. Bruckbauer, D. J. Zhou, D. J. Kang, Y. E. Korchev, C. Abell, and D. Klenerman, J. Am. Chem. Soc. **126**, 6508 (2004).
[190] M. J. Levene, J. Korlach, S. W. Turner, M. Foquet, H. G. Craighead, and W. W. Webb, Science **299**, 682 (2003).
[191] H. Rigneault, J. Capoulade, J. Dintinger, J. Wenger, N. Bonod, E. Popov, T. W. Ebbesen, and P. F. Lenne, Phys. Rev. Lett. **95**, 117401 (2005).
[192] S. H. Garrett, L. H. Smith, and W. L. Barnes, J. Mod. Opt. **52**, 1105 (2005).
[193] M. Moskovits, Rev. Mod. Phys. **57**, 783 (1985).
[194] K. Kneipp, H. Kneipp, I. Itzkan, R. R. Dasari, and M. S. Feld, Chem. Rev. **99**, 2957 (1999).
[195] S. Mahajan, J. J. Baumberg, A. E. Russell, and P. N. Bartlett, Phys. Chem. Chem. Phys. **9**, 6016 (2007).
[196] A. G. Brolo, E. Arctander, R. Gordon, B. Leathem, and K. L. Kavanagh, Nano Lett. **4**, 2015 (2004).
[197] J. R. Anema, A. G. Brolo, P. Marthandam, and R. Gordon, J. Phys. Chem. C **112**, 17051 (2008).
[198] T. H. Reilly, S. H. Chang, J. D. Corbman, G. C. Schatz, and K. L. Rowlen, J. Phys. Chem. C **111**, 1689 (2007).
[199] J. T. Bahns, F. N. Yan, D. L. Qiu, R. Wang, and L. H. Chen, Appl. Spectrosc. **60**, 989 (2006).

[200] A. Lesuffleur, L. K. S. Kumar, A. G. Brolo, K. L. Kavanagh, and R. Gordon, J. Phys. Chem. C **111**, 2347 (2007).
[201] S. M. Williams, A. D. Stafford, K. R. Rodriguez, T. M. Rogers, and J. V. Coe, J. Phys. Chem. B **107**, 11871 (2003).
[202] K. R. Rodriguez, S. Shah, S. M. Williams, S. Teeters-Kennedy, and J. V. Coe, J. Chem. Phys. **121**, 8671 (2004).
[203] J. V. Coe, S. M. Williams, K. R. Rodriguez, S. Teeters-Kennedy, A. Sudnitsyn, and F. Hrovat, Anal. Chem. **78**, 1384 (2006).
[204] J. V. Coe, K. R. Rodriguez, S. Teeters-Kennedy, K. Cilwa, J. Heer, H. Tian, and S. M. Williams, J. Phys. Chem. C **111**, 17459 (2007).
[205] S. Teeters-Kennedy, S. M. Williams, K. R. Rodriguez, K. Cilwa, D. Meleason, A. Sudnitsyn, F. Hrovat, and J. V. Coe, J. Phys. Chem. C **111**, 124 (2007).
[206] S. M. Williams, K. R. Rodriguez, S. Teeters-Kennedy, S. Shah, T. M. Rogers, A. D. Stafford, and J. V. Coe, Nanotechnology **15**, S495 (2004).
[207] E. Altewischer, M. P. van Exter, and J. P. Woerdman, Nature **418**, 304 (2002).
[208] A. G. Brolo, S. C. Kwok, M. D. Cooper, M. G. Moffitt, C. W. Wang, R. Gordon, J. Riordon, and K. L. Kavanagh, J. Phys. Chem. B **110**, 8307 (2006).
[209] D. J. Bergman and M. I. Stockman, Phys. Rev. Lett. **90**, 027402 (2003).
[210] C. Janke, J. G. Rivas, C. Schotsch, L. Beckmann, P. H. Bolivar, and H. Kurz, Phys. Rev. B **69**, 205314 (2004).
[211] J. Ji, J. G. O'Connell, D. J. D. Carter, and D. N. Larson, Anal. Chem. **80**, 2491 (2008).
[212] A. A. Tseng, Small **1**, 924 (2005).
[213] Y. H. Ye and J. Y. Zhang, Opt. Lett. **30**, 1521 (2005).
[214] J. Henzie, J. E. Barton, C. L. Stender, and T. W. Odom, Acc. Chem. Res. **39**, 249 (2006).
[215] J. Henzie, M. H. Lee, and T. W. Odom, Nature Nanotechnol. **2**, 549 (2007).
[216] M. H. Lee, H. W. Gao, J. Henzie, and T. W. Odom, Small **3**, 2029 (2007).
[217] B. D. Gates, Q. B. Xu, M. Stewart, D. Ryan, C. G. Willson, and G. M. Whitesides, Chem. Rev. **105**, 1171 (2005).
[218] V. Malyarchuk, F. Hua, N. H. Mack, V. T. Velasquez, J. O. White, R. G. Nuzzo, and J. A. Rogers, Opt. Express **13**, 5669 (2005).
[219] J. H. Wei and D. S. Ginger, Small **3**, 2034 (2007).
[220] Z. Jaksic, M. Maksimovic, D. Vasiljevic-Radovic, and M. Sarajlic, Sci. Sinter. **38**, 117 (2006).
[221] G. Ctistis, P. Patoka, X. Wang, K. Kempa, and M. Giersig, Nano Lett. **7**, 2926 (2007).
[222] W. A. Murray, S. Astilean, and W. L. Barnes, Phys. Rev. B **69**, 165407 (2004).
[223] E. M. Hicks, X. Y. Zhang, S. L. Zou, O. Lyandres, K. G. Spears, G. C. Schatz, and R. P. Van Duyne, J. Phys. Chem. B **109**, 22351 (2005).
[224] D. Sinton, R. Gordon, and A. G. Brolo, Microfluid. Nanofluid. **4**, 107 (2008).
[225] J. C. McDonald, Acc. Chem. Res. **35**, 491 (2002).
[226] A. De Leebeeck, L. K. S. Kumar, V. de Lange, D. Sinton, R. Gordon, and A. G. Brolo, Anal. Chem. **79**, 4094 (2007).
[227] T. Thio, H. J. Lezec, and T. W. Ebbesen, Phys. B, Condens. Matter **279**, 90 (2000).
[228] Q. J. Wang, J. Q. Li, C. P. Huang, C. Zhang, and Y. Y. Zhu, Appl. Phys. Lett. **87**, 091105 (2005).
[229] P. Marthandam and R. Gordon, Opt. Express **15**, 12995 (2007).
[230] N. C. Lindquist, A. Lesuffleur, and S.-H. Oh, Phys. Rev. B **76**, 155109 (2007).